METEOR-Berichte

Seismogenic faults, landslides, and associated tsunamis off southern Italy

Cruise No. M86/2

December 27, 2011 – January 17, 2012
Cartagena (Spain) – Brindisi (Italy)

S. Krastel
C. Adami, J. Beier, J. Bialas, S. Bigella, F. Chiocci, G. Crutchley, D. Cukur, B. Frey, L. Fu, F. Gross, S. Gurcay, J. Hempelt, S. Koch, G. Lüttschwager, F. Maisto, L. Masi, T. Matthiesen, A. Micallef, E. Morelli, C. Papenberg, D. Ridente, J. Schwab, A. Sposato. M. Urlaub, G. Wetzel, D. Winkelmann

Editorial Assistance:

DFG-Senatskommission für Ozeanographie
MARUM – Zentrum für Marine Umweltwissenschaften der Universität Bremen

2014

The METEOR-Berichte are published at irregular intervals. They are working papers for people who are occupied with the respective expedition and are intended as reports for the funding institutions. The opinions expressed in the METEOR-Berichte are only those of the authors.

The METEOR expeditions are funded by the *Deutsche Forschungsgemeinschaft (DFG)* and the *Bundesministerium für Bildung und Forschung (BMBF)*.

Editor:
DFG-Senatskommission für Ozeanographie
c/o MARUM – Zentrum für Marine Umweltwissenschaften
Universität Bremen
Leobener Strasse
28359 Bremen

Author:

Prof. Dr. Sebastian Krastel
GEOMAR Helmholtz-Zentrum
für Ozeanforschung Kiel
Wischhofstraße 1-3
24148 Kiel

Telefon: +49 431 600 2841
Telefax: +49 431 600 2941
e-mail: skrastel@geomar.de

Citation: S. Krastel, C. Adami, J. Beier, J. Bialas, S. Bigella, F. Chiocci, G. Crutchley, D. Cukur, B. Frey, L. Fu, F. Gross, S. Gurcay, J. Hempelt, S. Koch, G. Lüttschwager, F. Maisto, L. Masi, T. Matthiesen, A. Micallef, E. Morelli, C. Papenberg, D. Ridente, J. Schwab, A. Sposato. M. Urlaub, G. Wetzel, D. Winkelmann (2014) Seismogenic faults, landslides, and associated tsunamis off southern Italy- Cruise No. M86/2 – December 27, 2011 – January 17, 2012 – Cartagena (Spain) – Brindisi (Italy). METEOR-Berichte, M86/2, 49 pp., DFG-Senatskommission für Ozeanographie, DOI:10.2312/cr_m86_2

ISSN 2195-8475

Contents

1. Summary

The continental margins of southern Italy are located along converging plate boundaries, which are affected by intense seismicity and volcanic activity. Most of the coastal areas experienced severe earthquakes, landslides, and tsunamis in historical and/or modern times. The most prominent example is the Messina earthquake of Dec. 28, 1908 (Ms=7.3; 80,000 casualties), which was characterized by the worst tsunami Italy experienced in the historical time (~2000 casualties). It is, however, still unclear, whether this tsunami was triggered by a sudden vertical movement along a major fault during the earthquake or as a result of a giant marine slide initiated by the earthquake. The recurrence rates of major landslides and therefore the risk associated with landslides is also unknown. Based on detailed bathymetric data sets collected by Italian colleagues in the frame of the MaGIC Project (Marine Geohazards along the Italian Coast), we collected seismic data (2D and 3D) and gravity cores in three working areas (The Messina Straits, off Eastern Sicily, the Gioia Basin). A dense grid of new 2D-seismic data in the Messina Straits will allow to map fault patterns in great detail. One interesting outcome in this context is the identification of a set of normal faults striking in an EW-direction, which is almost perpendicular to the previously postulated faults. This EW-striking faults seem to be active. The area off eastern Sicily is characterized by numerous landslides and a complex deformation pattern. A 3D-seismic data set has been collected during the cruise using the so called P-cable in order to investigate these deformation patterns in detail. The new data will be the basis for a risk assessment in the working areas.

Zusammenfassung

Die Kontinentalhänge vor dem südlichen Italien liegen an konvergenten Plattenrändern, die eine intensive Seismizität und vulkanische Aktivität aufweisen. Ein Großteil der Küstengebiete wurde in historischen Zeiten und/oder in der jüngeren Vergangenheit von schweren Erdbeben, Hangrutschungen und Tsunamis getroffen. Das bekannteste Beispiel ist das Messina Erdbeben vom 28.12.1908 (Ms=7.3, 80.000 Opfer), das den größten Tsunami Italiens in historischen Zeiten zur Folge hatte (2000 Opfer). Es ist bisher jedoch unklar, ob der Tsunami als Folge einer vertikalen Bewegung entlang einer Störung oder durch eine submarine Hangrutschung ausgelöst wurde. Die Wiederholraten von großen Hangrutschungen sind ebenfalls unbekannt. Basierend auf bathymetrischen Daten, die unsere italienischen Kooperationspartner im Rahmen des MaGIC Projektes (MArine Geohazards along the Italian Coast) gesammelt haben, haben wir in drei ausgewählte Gebieten (Straße von Messina, östliches Sizilien, Gioia Becken) seismische Daten (2D und 3D) und Schwerelotkerne gewonnen. Ein dichtes Netz aus 2D-seismichen Linien in der Straße von Messina wird es ermöglichen, Verwerfungen in diesem Gebiet zu charakterisieren. Interessanterweise wurde auch ein Satz von aktiven Abschiebungen identifiziert, die in Ost-West Richtung streichen. Damit verlaufen sie fast senkrecht zu den bisher postulierten Verwerfungen in diesem Gebiet. Das Gebiet östlich von Sizilien ist durch zahlreiche Hangrutschungen und ein komplexes Deformationsmuster charakterisiert. In diesem Gebiet wurde mittels des sogenannten P-Cables ein 3D-seismischer Datensatz gesammelt, um die Deformationsstrukturen im Detail zu analysieren. Die neu gesammelten Daten stellen eine umfassende Datenbasis für eine Risikoabschätzung in den Arbeitsgebieten dar.

2. Participants

Name	Discipline	Institution
Krastel, S., Prof. Dr.	Chief Scientist	GEOMAR
Adamai, C.	Seismic	La Sapienza
Beier, J.	Seismic	GEOMAR
Bialas, J., Dr.	Seismic	GEOMAR
Bigella, S.	Seismic	La Sapienza
Chiocci, F.L., Prof. Dr.	Morphology	La Sapienza
Crutchley, G. Dr.	Processing	GEOMAR
Cukur, D., Dr.	Seismics	GEOMAR
Frey, B.	Weather technician	DWD
Fu. L.	Seismic	GEOMAR
Gross, F.	Seismic	GEOMAR
Gurcay, S.	Seismic	DEU
Hempelt, J.	Weather technician	DWD
Koch, S.	Seismic	GEOMAR
Lüttschwager, G.	Seismic	GEOMAR
Maisto, F.	Hydroacoustic	La Sapienza
Masi. L.	Seismic	GEOMAR
Matthiesen, T.	Technician	GEOMAR
Micallef, A. Dr.	Hydroacoustic	UB
Morelli, E., Dr.	Morphology	La Sapienza
Papenberg, C., Dr	Processing	GEOMAR
Ridente, D., Dr.	Neotectonics	CNR
Schwab, J.	Sedimentology	GEOMAR
Sposata, A., Dr.	Morphology	CNR
Urlaub, M.	Sedimentology	NOCS
Wetzel, G.	Technician	GEOMAR
Winkelmann, D., Dr.	Sedimentology	GEOMAR

CNR	National Research Council, Roma, Italy
DEU	Dokuz Eyül University, Izmir, Turkey
DWD	Deutscher Wetterdienst – Seewetteramt, Hamburg
GEOMAR	Helmholtz-Zentrum für Ozeanforschung Kiel (GEOMAR)
La Sapienza	Università "La Sapienza", Roma, Italy
NOCS	National Oceanography Centre Southampton, UK

3. Research Program

The main objective Meteor-cruise M86/2 was to investigate submarine hazards and their consequences in three selected areas off southern Italy (off Eastern Sicily, Messina Straits, Gioia Basin, Figs. 1, 2). Southern Italy is well known for its tectonic activity, submarine mass wasting, and tsunamis. The most prominent example is the 1908 Messina Earthquake (Ms=7.3) and an associated tsunami. It caused ~80.000 casualties and was accompanied by the worst tsunami Italy has experienced in historical time (~2.000 casualties). Run-up height was up to 11 m. It is, however, still unclear, whether this tsunami was triggered by a sudden vertical movement along

a major fault during the earthquake or as a result of a giant marine slide initiated by the earthquake. In addition, the eastern flank of the Etna volcano is in permanent movement, and it is of greatest importance to investigate the deformation pattern in order to analyze the stability of the volcano flanks.

In the frame of the MaGIC project (Marine Geohazards along the Italian Coast funded by the Italian Civil Protection Department) a detailed bathymetric data base was created as reference for compiling maps of geohazards at the seafloor. These maps were used for planning detailed investigations of selected areas by means of seismic investigations and sediment sampling during Cruise M86/2. Such measurements are not intended in the frame of the MaGIC Project. In close cooperation with our Italian partners, we selected 3 areas (The Messina Straits, off Eastern Sicily, the Gioia Basin) for our proposed detailed investigations in order to study submarine hazards off southern Italy (Figs. 1, 2).

Off Eastern Sicily

The main objective of the work off Sicily is to proof the hypothesis, whether the 1908 tsunami was triggered by a submarine landslide in an area off Eastern Sicily, as suggested by Billi et al. (2008). They identified a scarp as a possible source of the tsunami. Their outcome is based on the study of the tsunami arrival times (Platania, 1909; Baratta, 1910) and is supported by inspection of some published bathymetric data (Marani et al., 2004) and crustal-scale seismic profiles (Scrocca et al., 2004). This view, however, is doubted by Argnani et al (2009b). A dense net of high-resolution seismic data, however, is lacking, and final proof for the existence or non-existence of such a slide is missing. In addition, we would like to analyze the risk related to volcanic and non-volcanic landslides in this area. The specific objectives are:

- Analyze the submarine deformation pattern resulting from the downslope movement of the east flank of Etna volcano. The movement of the east flank of Etna volcano onshore is clearly documented by laser interferometry and direct GPS-measurements. The submarine deformation pattern, however, is unknown. Seismic data shall be used to investigate faults, folds and lineaments reflecting the deformation.
- Test of the hypothesis that the 1908 tsunami was triggered by a landslide in this area. Detailed 2D and 3D-seismic data and core data of the slide suggested by Billi et al (2008) are lacking. By combining seismic work and coring we propose a detailed investigation of this area in order to evaluate the presence of such a slide, and (if present) to determine its volume, age, structures, and dynamics as basis for the assessment of its tsunami potential.
- Mapping and analysis of volcanic and non-volcanic landslides. Existing morphological data show numerous landslides off Eastern Sicily. Especially volcanic landslides in form of major debris avalanches most likely represent a major hazard. E.g., Pareschi et al. (2006a) propose a major tsunami in the early Holocene triggered by a debris avalanche from Mt. Etna (Sicily, Italy) which entered the Ionian Sea in the order of minutes. Some offshore deposits were interpreted as debris avalanche deposits (Pareschi et al., 2006b) but their tsunami potential is heavily debated (Vigliotto, 2008). The volume of this debris avalanche is still highly speculative and, therefore, the hazard assessment difficult. We expect to identify additional major slides on a dense grid of seismic data.

Messina Straits

The main objective of the work in the Messina Strait is to identify the 1908 seismic source, in terms of presence of a coseismic seafloor rupture and of the likelihood of submarine failures triggered by ground shaking. Moreover, from a general point of view, an advanced understanding of sediment transport processes and neotectonic setting of the Messina Straits as well as the identification of the tsunami source represent a substantial parameter for the seismic/tsunamis hazard assessment in this area. The individual objectives are:

- Search for and identification of seismogenic faults. The location of the fault responsible for the 1908 earthquake is still a matter of debate. Previous investigations (e.g. Argnani et al., 2009a) tried to identify a potentially seismogenic fault, the Taormina Fault, along the coast between Taormina and Messina but were not successful. The re-analyses of all the available historical sources depict a complex framework of the arrival time of tsunami waves at different location along the coasts. Re-computation of arrival time indicates a source no more than 40 km to the South. This area, however, was not surveyed in detail until now.
- Identification of submarine failures, with special attention to the shallow-water, where slides would have a high tsunamogenic potential. Numerous slides were identified on the bathymetric data but their thicknesses and volumes are unknown. These values are important for assessing the tsunami potential of the slides. In addition, no detailed information about buried landslides are available for the Messina Straits.
- Analysis of sediment transport processes. Downslope sediment transport on the submarine slopes occurs in canyons or as catastrophic mass wasting events. The sedimentary pattern is further complicated by strong current controlled sediment transport in the Messina Strait. We want to estimate the importance of the different processes and investigate the factors and processes controlling sediment transport.

Gioia Basin

The Gioia Basin is characterized by major submarine canyons and numerous slides. A landslide at one of the canyon heads triggered a tsunami in 1977. Major slides further downslope seem to be characterized by well pronounced glide planes. Due to relatively simple setting, this working area represents a good place to study the history of submarine landsliding and associated hazards. The specific aims are:

- Occurrence and distribution of slides: Do they represent a major hazard and risk? We want to study the dynamics of selected slides and estimate their recurrence rate in order to asses associated hazards. Special emphasis will be put on buried slides, which are known from the area but not well mapped and understood.
- Tectonic control of canyon evolution. Detailed morphological investigations of the canyons show a large variability with straight and meandering sections. Seismic data shall be used to decipher the controlling factors responsible for the canyon morphology.

Methods

Acoustic data were collected with the hydroacoustic systems of RV Meteor and the GEOMAR high-resolution seismic system. A GI-Gun acted as source. 2D-seismic data were collected using a 200m-long 128-channel digital Geometric GeoEel-streamer.

We deployed the GEOMAR P-Cable seismic system to collect 3D-seismic data in a 4*8km wide box east of Mount Etna. This system uses the same streamer segments as the 2D-system. The P-Cable is a cost-efficient low-fold high-resolution 3D-seismic acquisition system. It consists of sixteen 12.5m long mini-streamers that are towed less than 10 m apart resulting in an inline separation of less than 5 m. The system generates data with 3-6 m horizontal and 1-2 m vertical resolution.

Only minor problems occurred during the cruise. We had some delays due to an electrical problem with the p-cable. Strong winds also forced us to repeat several lines during the 3D-survey. Due to the extremely complicated pattern east of Sicily we extended this part of the program a bit while data collection in the Gioia Basin was reduced. A very valuable data- and sample set of sediment cores in combination with seismic (2D and 3D) and hydroacoustic data will allow investigate geohazards off southern Italy.

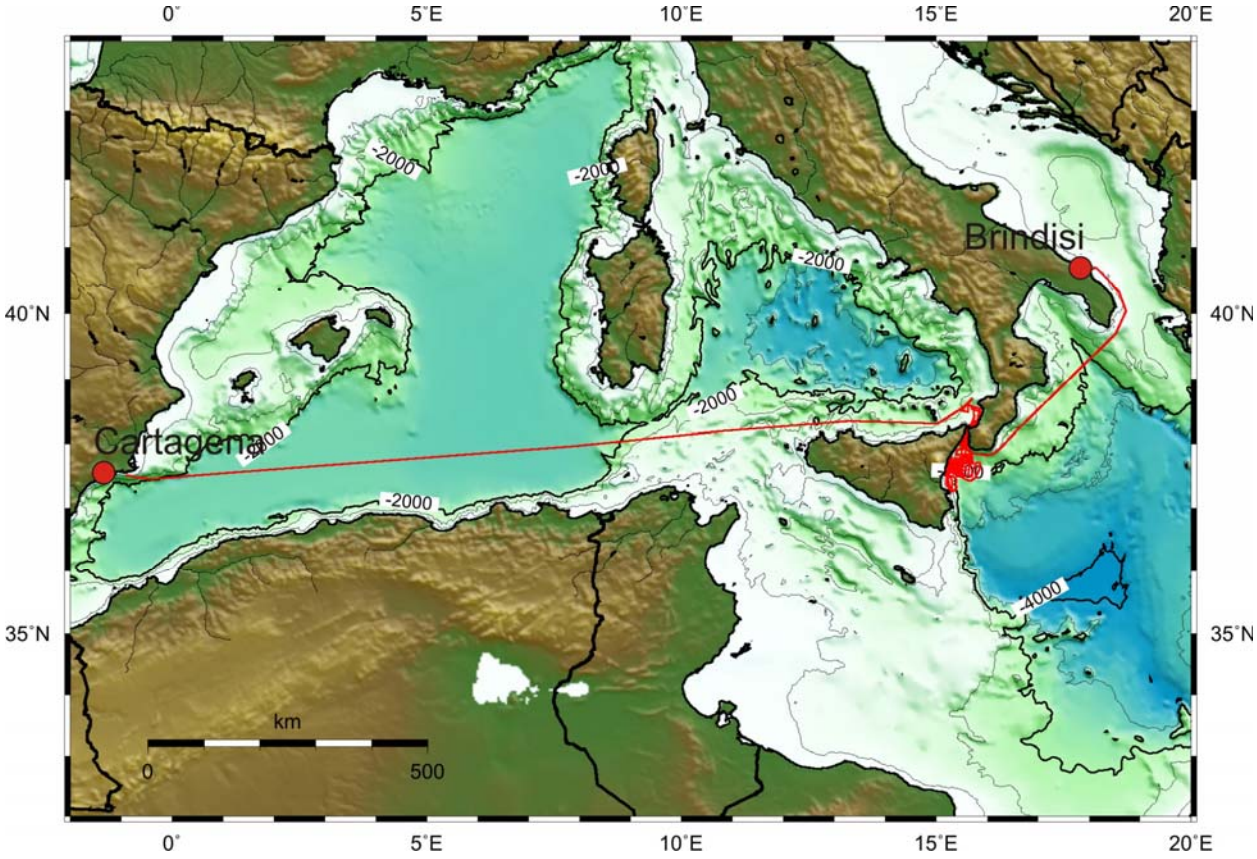

Fig. 1 Cruise track of Cruise M86/2. Details of the working area are shown on Fig. 2.

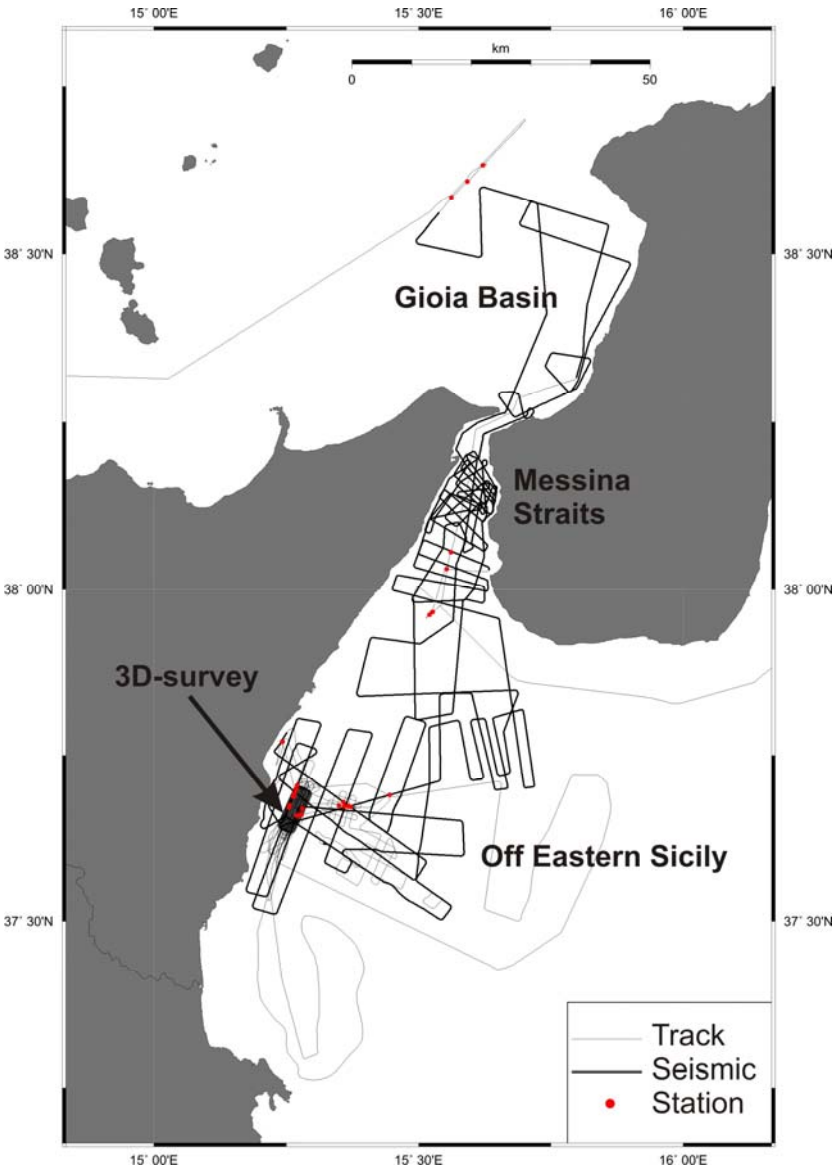

Fig. 2 Track plot of the working area.

4. Narrative of the Cruise

The entire scientific party arrived in Cartagena on December 26th and directly boarded RV Meteor. The scientific crew of RV Meteor-CruiseM86/2 included 14 scientists from the Helmholtz Centre for Ocean Research Kiel (GEOMAR) and the Cluster of Excellence 'The Future Ocean' (Kiel), six scientists from Univesità di Roma "La Sapienza", two scientists from the 'National Research Council' in Rome, and one scientist each from the 'National Oceanography Centre Southampton', the 'Universitat de Barcelona', and the 'Dokuz Eylul Universty' in Izmir, as well as two technicians from the 'German Weather Service'.

RV Meteor left port on December 27th as scheduled at 10:00h under sunny skies and a light breeze. Weather on the transit to our first working area was variable with wind speeds up to force 7 reducing the speed of Meteor to 8 knots for some periods. The transit was used for meetings and setup of the equipment.

RV Meteor entered Italian waters on December 29th at 14:15h. This was the start of the scientific program by switching on the hydroacoustic systems.

We arrived in our first working area (Gioia Basin) on December 30th at 10:00h. Work in this area started with a coring profile (Stations M862_01 to 03) across a landslide visible in

bathymetric data. Two of the 5m-long gravity corers were completely filled, while the third recovered about 3,50m of sediments. Clear slide deposits were recovered in the first core; the undisturbed drape is only a few dm. The other two cores were taken next to the slide and above the headwall and show undisturbed deposits. The first station was also sampled with the giant box corer; in addition a sound velocity profile was recorded for the hydroacoustic systems. The night was used for a first 2D-seismic survey with a 1.7 l GI-Gun and a 200m-long 128 channel streamer. Several canyons/channels were crossed at different locations. They show clear levee structures. Landslide deposits are widespread. We left this first working area on December 31st early morning. While collecting seismic data, we entered the Messina Straits. 2D-seismic data were collected across potential faults in the Messina Straits until January 1st in the afternoon. The main aim was to identify the fault being responsible for the 1908 earthquake. The support by local authorities, especially the traffic control, was outstanding and allowed us to run our survey as planned. The survey was shortly interrupted in the morning of the December 31st due to problems with a fishing line, which was picked up by the streamer.

Seismic data collection was continued east of the Etna until January 1st in the morning. A grid of 2D-seismic lines was collected in order to define targets for the 3D survey. Weather on January 1st and 2nd was very nice and allowed spectacular views of Etna volcano. Seismic data acquisition close to the coast line was limited to daytime due to intense fishing activities. The streamer picked up fishing lines twice during the survey.

January 3rd was used for sediment sampling while changing the seismic system to a 3D-mode. Three cores (M862-04 to 06) were taken in a small basin (ca. 5 km diameter) beneath a major landslide scarp. Hydroacoustic data show a complex pattern of landslide deposits of varying sizes. The cores were located with the aim to sample several of these deposits. Afterwards four cores (M862-07 to M862-10) were taken on and between elongated ridges in about 500m water depth. It is unclear whether these ridges represent deformation patterns as a result of the moving Etna flanks, landslide blocks, surface expressions of deeper tectonic features, or anything else. All cores brought good recoveries except for the one on the Chaincone Fan (M862-10), which was empty. The night was used for hydroacoustic surveys of small sedimentary basins.

The above mentioned ridges were also chosen as target for a 3D-survey with the so called P-Cable. The P-Cable is a cost-efficient low-fold high-resolution 3d-seismic acquisition system developed by VBPR, NOCS and the University of Tromsø and recently adapted and extended by GEOMAR. It uses the same streamer segments as the 2D-seismic system. Usually it consists of sixteen 12.5-m long streamer that are towed 10 m apart resulting in an inline separation of 5 m. Due to technical problems only 13 streamers could be deployed. Deployment was planned for January 4th in the morning but was delayed due to technical problems. Hence January 4th was used to collect additional sediment samples of a channel floor and a sedimentary basin (M862-11 to 13). Thereafter 4 Ocean Bottom Seismometers were deployed in the box for the 3Dd-survey. Due to further delays in preparation of the P-Cable, the night was used for an additional hydroacoustic survey extending the existing bathymetric data coverage.

Deployment of the P-Cable started on January 5th at 06:00h in the morning. The erupting Etna in the background offered a spectacular setting for the deployment (Fig. 3). Data acquisition started around 09:30h. The start was very smooth but during the night the wind increased with gusts up to force 8. Nevertheless data quality was good and the data acquisition was continued until January 6th in the evening. At this point the wind was so strong (gusts up to force 10) that it was impossible to keep the vessel on the profiles. During a turn, the wire running to the starboard trawl doors was entangled with the door itself thereby losing any shearing forces. At that point

we decided to retrieve the entire system because even stronger winds were predicted for the night and the morning of January 7th. Indeed gusts up to Beaufort 10 were measured on January 7th. However, coring was still possible. Three cores were recovered crossing a landslide feature in the 3D-Box (M862-14 – 16). After that we tried to core some postulated mud volcanoes close to the shore (M862-17 and 18). We used a gravity corer and the giant box corer but the only material recovered from the sea floor was some heavily cemented sediments and/or volcaniclastics in a core catcher from a gravity core. Coring was shortly interrupted because the ship received a call from the coast guard to support a rescue operation for a wind surfer. After the surfer was picked up by a small fisher boat, we continued our work. In the meantime the wind was slightly calming down. Hence we decided to deploy the 3D-seismics despite some gusts up to force 9. Deployment was quick and successful.

All components of the 3D-system worked without any problems until early morning on January 10th. At that time a problem with the GPS-receives on the trawl doors and a gun error forced us to interrupt the survey. After finishing the gun repairs, the system worked but an hour later (ca. 11:00h) parts of the streamer lost connection to the deck unit. The recovery of the system showed some broken eyelets at the t-connectors, which are used for the rope keeping tension from the data cable. As a result two of the data cables were heavily stretched and needed to be replaced. Afterwards the system was successfully deployed but another failure occurred around 20:00h the same day. Parts of the streamers again lost connection to the deck unit. This time the problem could be solved by replacing one t-connector. The entire system was back in the water around 22:30h. All tracks of the 3D-box were collected around noon on January 11th. However, due to strong winds during major parts of the survey some gaps were still open and we continued the seismic 3D-survey until January 12th at 08:30h in order to fill these gaps. In total we run about 700 km of profiles in the 3D-Box and fired more than 110.000 shots. Hence this part of the ocean floor and the underlying structures is one of the best imaged sections worldwide. Retrieval of the gear was fast; afterwards the Ocean Bottom Seismometer were released and picked up without any problems. A first quick look at the OBS section does not only show records of the shots but also prominent signals which seem to be related to the eruption of Mt. Etna on December 5th.

The early afternoon was used for sediment coring. A first core in a landslide scar (M862-19) brought more than 7 m sediments on deck. Two additional cores were taken on ridge structures of the 3D-box, both with core length between 4 and 5 m (M862-20 and 22), while a forth core (M862-21) immediately next to one of these ridges was empty. It is not easy to explain that the elevated ridge structures are covered by soft sediments, while the seafloor next to the ridges is very hard.

The 2D-seismic was deployed early evening on January 12th. Some additional profiles were collected east of the Etna in order to further analyze the regional deformation patterns. Seismic surveying was continued on January 13th with several crossings of a prominent morphological step at the southernmost part of the Messina Straits. This morphological step is the most prominent active fault in the entire survey area and can be traced for almost 20 km. The night and the following day were used for additional lines in the Messina Straits before we passed through the Straits in order to collect 2D-seismic data off Scilla and Gioia-Tauro. A subaerial landslide entering the sea occurred in February 1783 close to Scilla and triggered a local tsunami, which killed 1500 persons. The subaerial landslide may be related to submarine landsliding activity. The aim of the profiles off Gioia-Tauro was to investigate submarine canyons. The seismic gear was recovered on January 15th and we started a short transit through the Straits in order to take cores in the Messina Canyon. Only a very few positions were

approved in the Messina Straits by the authorities due to abundant submarine cables. Messina Canyon was very difficult to core. Three gravity cores (M862-23 to 25) did not result in any recovery and one of the cores was bent. Hence we took a final box corer (M862-26) recovering some sediments and human waste. The seismic 2D-system was deployed for the last time on January 15t at 17:00h. Some final profiles were shot in the southernmost part of the Messina Straits. All equipment was successfully recovered on January 16th at 02:00h. Thereafter we started our transit to Brindisi. The hydroacoustic systems were switched off on January 16th at 07:40h. RV Meteor arrived in Brindisi on January 17th at 08:30h.

Meteor-Cruise M86/2 was a great success. We collected about 740 nm of seismic 2D-lines in exceptional quality. An 8 x 4 km large area was successfully surveyed in 3D with the P-Cable. About 80 m of cores were recovered at 26 stations. In addition hydroacoustic data were collected along all seismic profiles and transits. The new data will allow an in depth investigation of submarine hazards off Southern Italy.

Fig. 3 P-cable deployment in front of the erupting Etna on January 5th.

5. Preliminary Results

5.1. Hydroacoustics

5.1.1. Bathymetric mapping

(A. Micallef, J. Schwab, and Shipboard Scientific Party)

Technical description

During Cruise M86/2 the hull-mounted Kongsberg Simrad systems EM122 and EM710 were used for bathymetric mapping. The deep water system EM122 was operated continuously during all seismic surveys but also on transit routes in a 24 hour schedule. The shallow water systems EM 710 was recorded in areas with water depths shallower than 1000m.

The EM122 system allows an accurate bathymetric mapping down to full ocean depth. The EM122 is a successor of the EM120, which was operated on RV Meteor from 2006 to 2010. It uses the same transducers as the EM 120 but with new electronics and software.

Basic components of the system are two linear transducer arrays in a Mills cross configuration with separate units for transmitting and receiving. The nominal sonar frequency is 12 kHz with an angular coverage sector of up to 150° and 864 soundings per ping. Compared with the EM 120 the EM 122 has up to four times the resolution in terms of sounding density through inclusion of multiping capability and more than twice the number of detections per swath. In

typical ocean depths a sounding spacing of about 50 m across and along is achievable (dos Santos Ferreira et al, 2011). The achievable swath width on a flat bottom will normally be up to six times the water depth dependent of the roughness of the seafloor. The angular coverage sector and beam pointing angles may be set to vary automatically with depth according to achievable coverage. This maximizes the number of usable beams. The beam spacing is normally equidistant, but an equiangular mode is also available. Using the detected two-way-travel-time and the beam angle known for each beam, and taking into account the ray bending due to refraction in the water column due to sound speed variations, depths are calculated for each beam. A combination of amplitude (for the central beams) and phase (slant beams) is used to provide a measurement accuracy practically independent of the beam pointing angle. Beside the depth values, the EM122 provides also backscatter information and pseudo-sidescan images.

The EM 710 multibeam echo sounder is a high to very high resolution seabed mapping system. The minimum acquisition depth is from less than 3 m below its transducers, and the maximum acquisition depth is specified down to 2000 m. However, during the cruise it turned out that the quality of the data degrades in water depths deeper than 1000 m. The acrosstrack coverage (swath width) can reach 5.5 times the water depth. During the cruise, the swath width was adjusted manually to get the best compromise between coverage and data quality with changing water depth and sea state. The EM 710 operates at sonar frequencies in the 70 to 100 kHz range. The transmit fan is divided into three sectors to maximize range capability but also to suppress interference from multiples of strong bottom echoes. The sectors are transmitted sequentially within each ping, and uses distinct frequencies or waveforms. The alongtrack beamwidth of the system installed on RV Meteor is 1 degree. A ping rate of up to 25 per second is possible. The transmit fan is electronically stabilized for roll, pitch and yaw. The EM 710 on R/V Meteor has a reception beamwidth of 1 degree as well. The number of beams is 256 or 400 (high resolution mode). The beamspacing may be set to equiangular or equidistant. The receive beams are electronically roll stabilized. A combination of phase and amplitude bottom detection algorithms is used in order to provide soundings with the best possible accuracy. Additionally, an integrated seabed acoustical imaging capability is included as standard. A real time display window for water column backscatter is also available.

As bathymetric maps were available by our Italian colleagues, only some quick processing was done onboard using the open source MultiBeam software, which includes automatic and interactive editing and gridding. Final maps were produced by using the Global Mapper software. A map of the newly acquired data in the Messina Straits and East of Sicily is shown on Fig. 4.

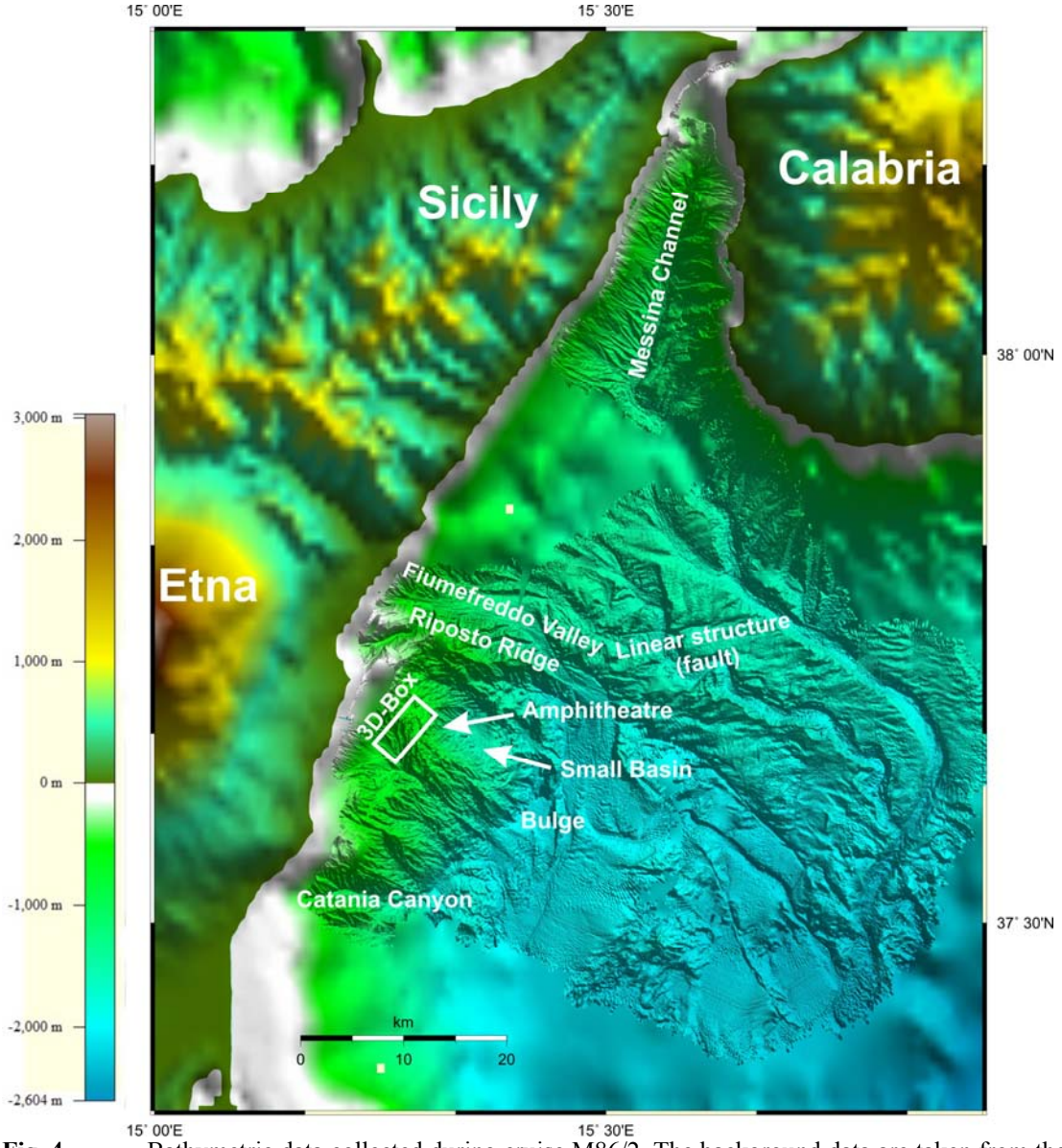

Fig. 4 Bathymetric data collected during cruise M86/2. The background data are taken from the GEBCO 0.5 minute grid.

Preliminary results

As maps were already available and analyzed by our Italian colleagues, only a very brief description of some features is given here. The central part of the Messina Straits is characterized by the prominent Messina channel. Abundant tributary channels are visible both on the Sicilian and Calabrian side (Fig. 4). The tributaries on the Sicilian side show a relative regular pattern and straight canyon courses. The Calabrian side is much more complex. Several canyons show anomalies (e.g. change in the course of the canyon), which is often associated with a concentration of slides. These anomalies may be the result of active faults. A prominent straight feature is found at the southernmost part of the Messina Straits (Fig. 4). This feature is clearly visible in the bathymetry and crosses several canyons. It has a length of ~20km. This feature was surveyed by a dense net of seismic 2D-lines as the bathymetry suggest the feature to be an active fault scarp (see chapter 5.2.)

The area east of Sicily shows a very complex morphological pattern. A very prominent feature is a major amphitheater-like incision east of Etna volcano (Fig. 5). This incision is most

likely formed by a major landslide though no obvious deposits are found on the bathymetric data; hence it seems to be an old feature. A small basin with a diameter of ~5km and a water depth of ~1600m is located east of the amphitheater-like incision, which collected the deposits of several smaller landslides (see Parasound section 5.1.2.). Several deeply incised channels are clearly visible in the bathymetry. The area between Catania Canyon and Riposto Ridge corresponds to an onshore area of Etna, which is characterized by ongoing deformation. Some radial ridges (e.g. in the 3D-box) may be formed by this deformation. Hence these ridges were chosen as one main target of the 3D-seismic box.

5.1.2. Sediment echo sounding

(F. Gross, J. Beier, and Shipboard scientific party)
During cruise M86/2 the hull-mounted sediment echo sounder system Parasound was used in a 24 hour watch mode. The system was mainly used to image sediment depositional processes.

System description
Since March 2006 the new Parasound system P70 is installed on RV Meteor. The system uses the parametric effect, which occurs when very high (finite) amplitude sound waves are generated. If two waves of similar frequencies are generated simultaneously, also the sum and the difference of the two primary frequencies are emitted. For the Parasound System, 18 kHz is one fixed primary frequency, which is generated by a transducer of ~ 1m length within a beam of 4.5°. The second primary frequency can be varied between 18.5 and 24 kHz, resulting in difference frequencies from 0.5 to 6.0 kHz. This signal travels within the 18 kHz beam, which is much narrower than e.g. a 4 kHz signal, emitted from the same transducer directly (30°). Therefore, a higher lateral resolution can be achieved, and imaging of small scale structures on the sea floor is superior to conventional systems. As another consequence, the signal bandwidth is also increased, and much shorter signals can be generated with improved vertical resolution. Due to the narrow beam, it is necessary to control beam direction, to compensate the ship's movement, and to send the energy vertically downwards. The system treats three signals separately: the primary high frequency signal (18 kHz; PHF), the secondary low frequency signal (selectable 0.5 to 6.0 kHz; SLF) and the secondary high frequency (selectable 36.5 to 42 kHz; SHF). We selected 4 kHz as SLF and 40 kHz as SHF. All three signals are recorded separately. Alternatively, also exclusively a low frequency signal (PLF; 3 or 12 kHz) can be emitted at much lower energy levels, if sound emission energy levels have to be limited (e.g. for mammal protection).

The Parasound system uses minimum three different computer systems. Two of them control real-time signal generation and data acquisition through a Linux and a Windows system. The third PC is available for the operator. This Operator-PC hosts the Hydromap Database Server, the Hydromap Control Software and the ParaStore 3 Software. The Hydromap Control Software is responsible for all system settings and for communication with the real-time computers. The ParaStore Software Package is used for visualization, online processing, and data storage. Data can be stored in the Parasound ASD format, but also in the more common PS3 or SEG-Y formats. Several windows can be opened to display different signals (PHF, SLF, SHF) with different scaling and/or processing parameters. This allows optimizing the windows for specific purposes, as e.g. imaging of the upper 20 m of sediments to select optimal coring locations, to

choose a full penetration plot, which also allows coverage of the topography, or to study the complete water column.

The system can be used in the single pulse mode, when a single pulse is emitted and the water column and sediment response are recorded before the next pulse is sent, or in the pulse train or quasi equidistant mode, by which the two-way travel time of the signal in the water column is used to emit additional signals. Depending on water depth, the signal density can be increased by as much as a factor of 16. At the beginning of the cruise we mainly operated in a single pulse mode. This was changed after the first week to a pulse train mode in order to acquire data with better lateral resolution. The Simrad EM122 depth was usually used as system depth. This setup worked very well during the cruise.

System crashes were significantly less infrequent than during previous cruises. Time synchronization errors between the different components occurred at the beginning of the cruise after restarts. This problem was usually solved by repeated restarts. CM recovery actions were very frequent but did not harm data acquisition. Both problems were solved after a remote maintenance by STN Atlas.

Preliminary results:

Parasound data were recorded along all seismic profiles and on all transits. A few examples are shown in the following.

Fig. 5 illustrates a profile trough a little basin approximately 15 km off the eastern coast of Mt. Etna. It is crossing gravity core locations M86/2-005 and M86/2-012. The basin, located in about 1550 m water depth, is confined by a steep 250m-high flank to the south and a more gentle ~70m-high flank to the north. Maximum penetration is ~60 m within the basin. Due to the relatively steep slopes, the sedimentary structures of the margins are only poorly resolved. Well stratified sediments in the basin are interrupted by lenticular shaped, transparent units (Fig. 5). These units represent mass transport deposits, which are also found in some of the cores in that area (see chapter 5.5.3., e.g. core M86/2-007). The mass transport deposits are covered by undisturbed sediments. The high reflective layers within the basin may correspond to widespread tephra layers, also visible in most of the already opened cores.

The profile shown on Fig. 6 is orientated from south-southeast to north-northwest and crosses a linear morphological step identified in the bathymetric data (see chapter 5.1.1). This profile clearly shows that the morphological step is the surface expression of a complex pattern of normal faults. The faults show a clear offset of sedimentary units directly at the sea floor suggesting that these faults are still active. It is interesting to note that the strike direction of the fault system is approximately E-W, which is perpendicular to all previously postulated faults in the Messina Straits.

Parasound profile P305 (Fig. 7) was collected about 5 km off the eastern coast of Mount Etna and is orientated southwest to northeast. It crosses a morphological high with a water depth of ~ 440 m. The upper part of the sedimentary succession (down to ~20 m beneath the sea floor) shows several incisions and chaotic deposits, which are interpreted as landslide scars and corresponding mass transport deposits. This area seems to be characterized be abundant but small slope failures. The lower sedimentary succession shows well stratified continuous reflectors of varying amplitudes. Gravity core locations M86/2-14-16, 19 are within the profile and marked by black arrows. The aim of these cores was to sample young landslide deposits.

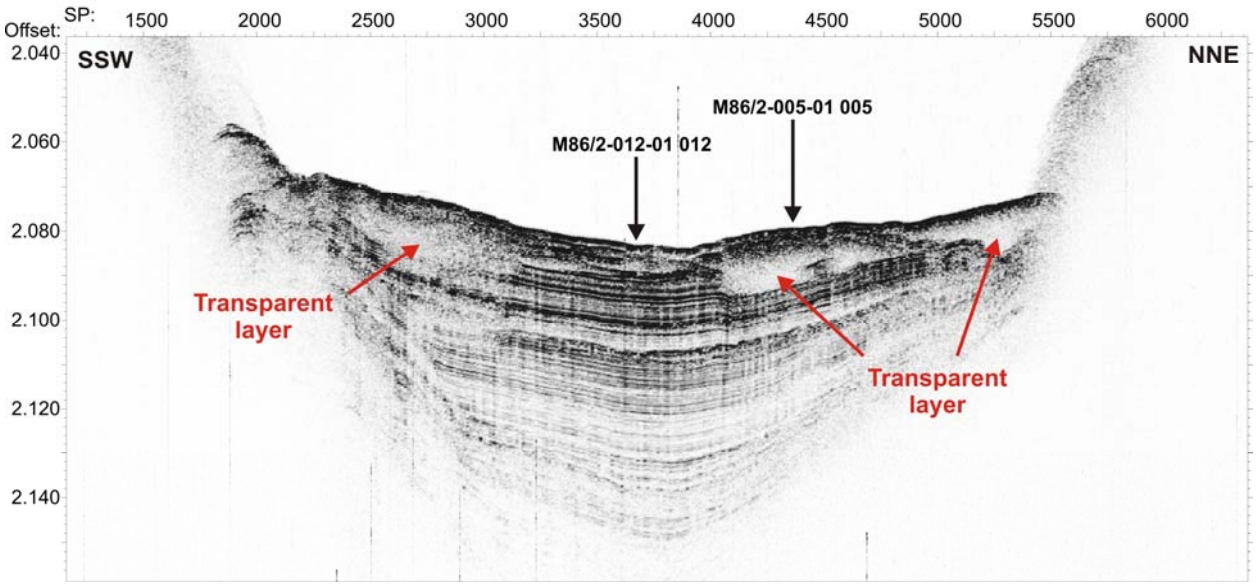

Fig. 5 Parasound profile P007 crossing a little basin 15 km offshore the eastern flank of Mt. Etna. The transparent, lenticular-shaped layers are interpreted as mass transport deposits. Core locations M86/2-005-01 and M86/2-012-01 are shown by black arrows. Location of profile is shown on Fig. 17 (chapter 5.2.3.).

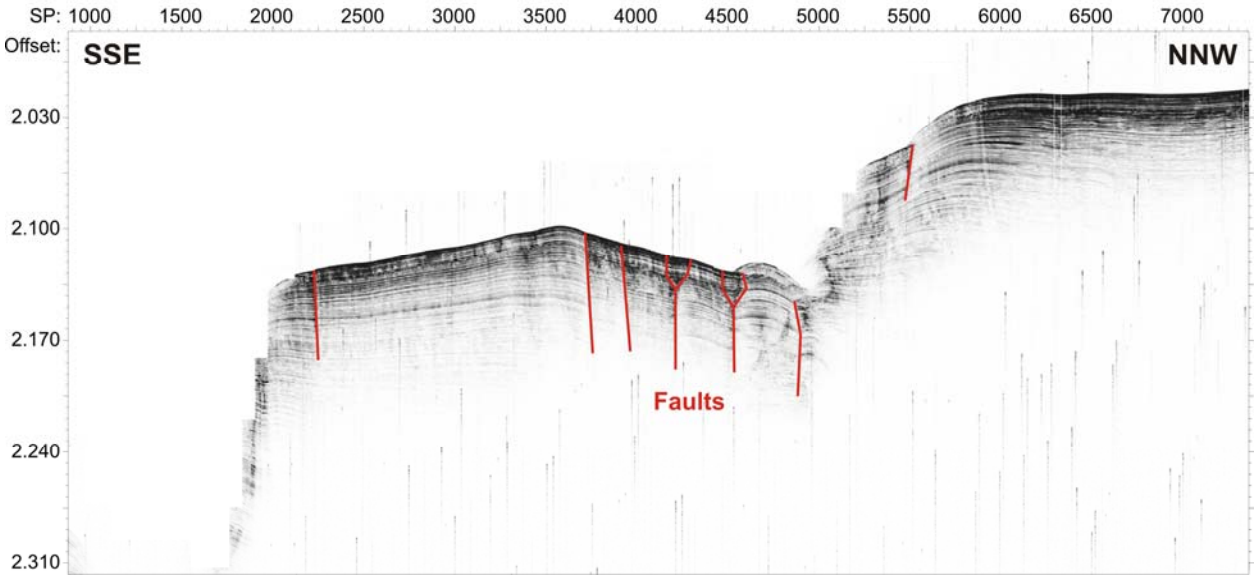

Fig. 6 Parasound profile P807 crossing a prominent morphological step identified in the bathymetric data. Faults are marked as thin red lines. Location of profile is shown on Fig. 17 (chapter 5.2.3.).

Fig. 8 shows a Parasound profile (P5512) collected during the 3D survey. It runs in a SSW-NNE direction and is located about 6 km offshore the eastern flank of Mount Etna. Three prominent highs are visible on this profile, which are part of elongated radial features identified in the bathymetric data. The internal structure of these features is poorly resolved. The area between the blocks is characterized by a strong smooth sea floor reflector with almost no sub-bottom penetration. The north-eastern part of the profile shows good penetration and some stratified sediments. The origin of the morphological highs is unclear. They may represent deformation patterns, rafted blocks, or current induced features. One aim of the 3D-survey was to distinguish between these possibilities.

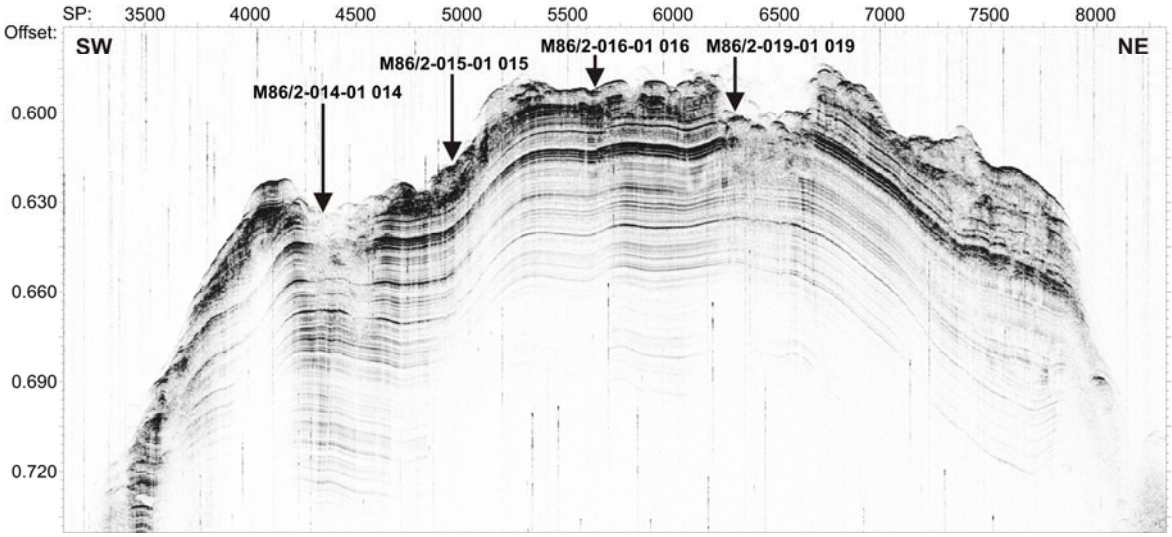

Fig. 7 Parasound profile P305 crossing a morphological high with several indications for submarine mass wasting. Core locations M86/2- 14-16, 19 are marked by black arrows. Location of profile is shown on Fig. 17 (chapter 5.2.3.).

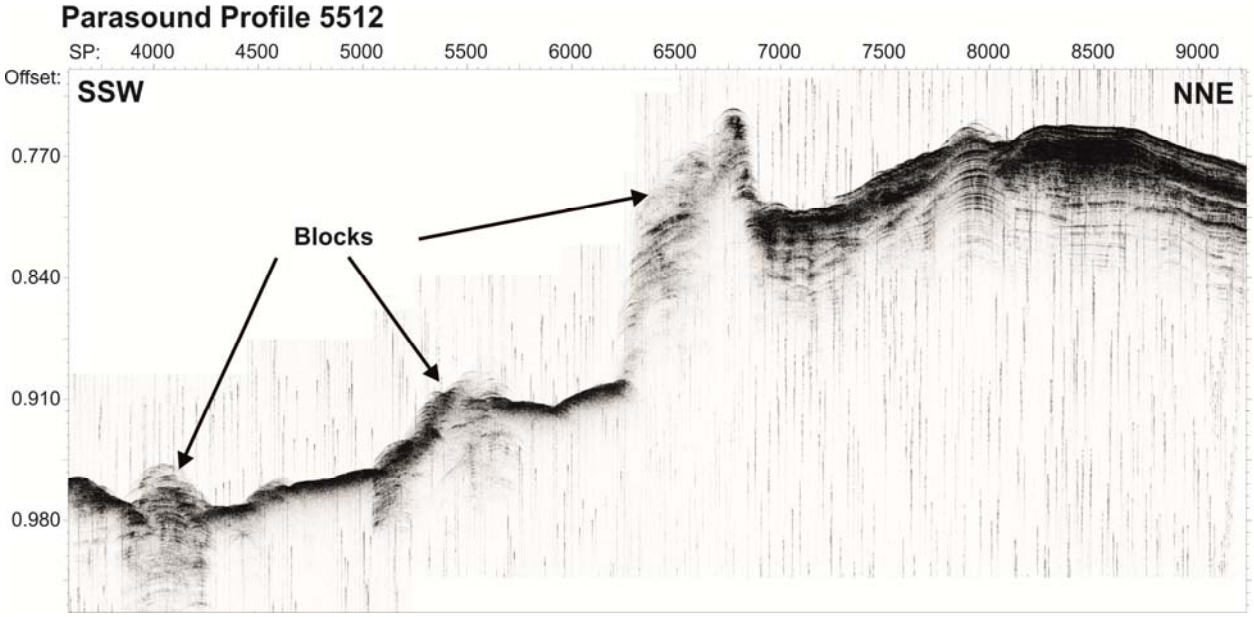

Fig. 8 Parasound profile P5512 collected during the 3D-survey. It crosses three blocks, which may represent deformation patterns, rafted blocks, or current induced features. Location of profile is shown on Fig. 17 (chapter 5.2.3.).

5.2. High resolution 2D multichannel seismic profiling

(J. Beier, J. Bialas, G. Crutchley, D. Cukur, L. Fu, F. Gross, S. Gurcay, S. Koch, G. Lüttschwager, C. Papenberg, J. Schwab)

5.2.1. Introduction

During Cruise M86/2 equipment of the Helmholtz Centre for Ocean Research Kiel (GEOMAR) was used to acquire high-resolution multichannel seismic data. The aim was to resolve small scale sedimentary structures and closely spaced layers on a meter scale, which can usually not be resolved by means of conventional seismic systems. A 1.7l GI-Gun was used as source during the cruise. Data were recorded with a Geometrics GeoEel digital streamer. Figs. 9

and 10 give an outline of the system setup as it was used during R/V Meteor Cruise 86/2. Tab. 1 lists the individual setting for each profile.

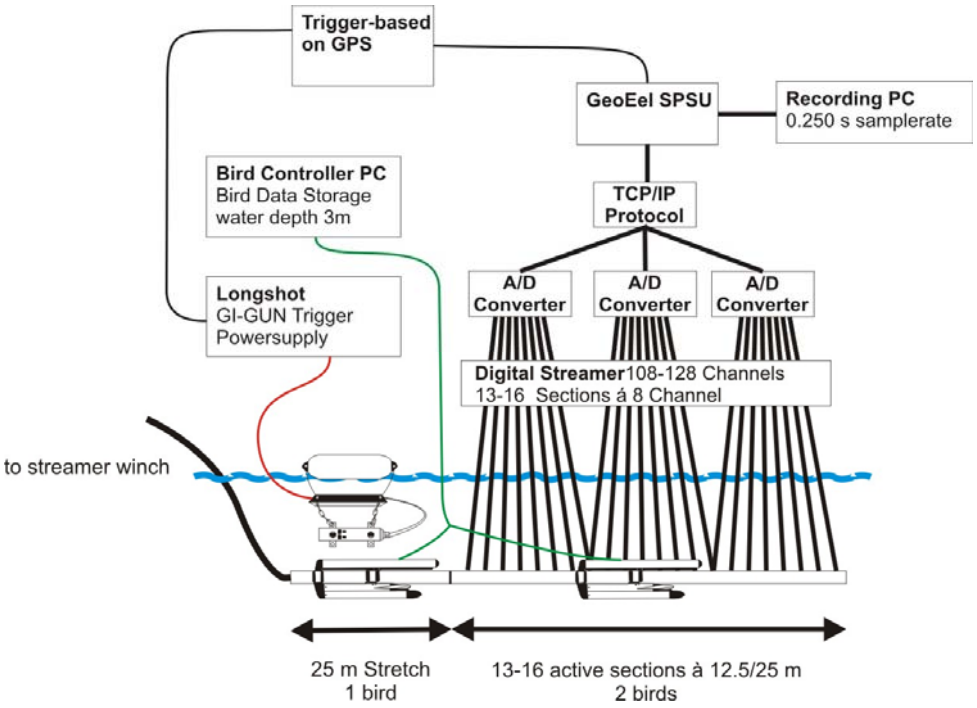

Fig. 9 Setup of 2D-seismic system during Cruise M86/2.

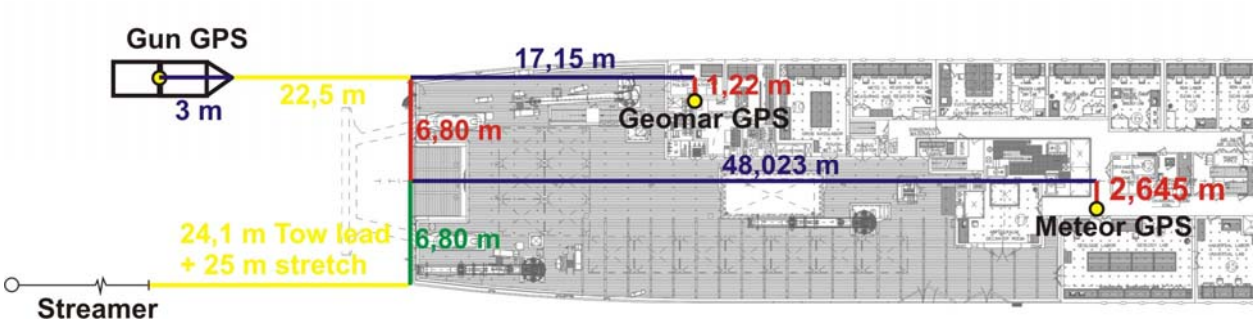

Fig. 10 Deck and seismic gun setting during Cruise M86/2.

Table. 1: Source and receiver settings for individual profiles.

Profile	Source, mode, shooting rate (s)	Streamer	Birds
101-111	1.7l GI-Gun, harmonic mode, 4-6s	128 channels, 25m-stretch, 14 12.5m sections, 2 25m sections	End stretch. Section 5, Section 12
201-248	1.7l GI-Gun, harmonic mode, 4-6s	120 channels, 25m-stretch, 13 12.5m sections, 2 25m sections	End stretch. Section 5, Section 12
249-307	Mini GI-GUN 0.2, true GI, 2.5-5.5s	112 channels, 25m-stretch, 13 12.5m sections, 1 25m sections	End stretch. Section 5, Section 12
401-408	1.7l GI-Gun, harmonic mode, 4-6s	120 channels, 25m-stretch, 13 12.5m sections, 2 25m sections	End stretch. Section 5, Section 12
601-1108	1.7l GI-Gun, harmonic mode, 4-6s	104 channels, 25m-stretch, 13 12.5m sections	End stretch. Section 5, Section 10

5.2.2. System components

Seismic sources

During seismic surveying a standard GI-Gun was used as source; it was shot in a harmonic mode (2 * 1.7 l). The GI-Gun was deployed with the port side crane and towed ~22.5 m behind the ship's stern (Fig. 10). The-GI-gun was connected to a bow with the GI-Gun hanging on two chains 70 cm beneath. An elongated buoy, which stabilized the guns in a horizontal position at a water depth of ~2 m, was connected to the bow by two rope loops. The Injector of the GI gun was triggered with a delay of 10 ms with respect to the Generator signal, which basically eliminated the bubble signal. The gun was shot at 200 bar. Shooting intervals varied between 4 and 6 seconds (depending on water depth) resulting in a shot point distance of 10-15 m at 5 knots. The gun worked very reliable during the entire cruise except for some problems with the umbilical.

Streamer-systems

A digital streamer (Geometrics GeoEel) was used for receiving the seismic signals. The system consists of a tow cable (80 m, 24 m in the water), one stretch section (25 m) and 13 - 16 active sections (each 12.5/25 m long). Most of the sections had a length of 12.5 m. At the beginning of the survey, a few profiles have been collected with one or two 25 m sections at the end of the streamer (Tab. 1). An active section contains 8 channels (channel spacing of 1.56 m for 12.5 m sections and 3.25 m for the 25 m sections) resulting in 112-128 channels within the total streamer (see Tab. 1). One AD digitizer module belongs to each active section. These AD digitizer module are small Linux computers. Communication between the AD digitizer modules and the recording system in the lab is via TCP/IP. A repeater was located between the deck cable and the tow cable (Lead-In). The SPSU manages the power supply and communication between the recording system and the AD digitizer modules. The recording system is described below. Three birds were attached to the streamer (see below). Designated streamer depth was 3 m. A small buoy was attached to the tail swivel.

Bird Controller

Three Oyo Geospace Bird Remote Units (RUs) were deployed at the streamer. The locations of the birds are listed in Tab. 1. All RUs have adjustable wings. The RUs are controlled by a bird controller in the seismic lab. Controller and RUs communicate via communication coils nested within the streamer. A twisted pair wire within the deck cable connects controller and coils. Designated streamer depth was three meters. The RUs thus forced the streamer to the chosen depth by adjusting the wing angles accordingly. The birds were deployed at the beginning of a survey but no scanning of the birds was carried out during the survey because bird scans caused major problems with acquisition system. The birds worked very reliable and kept the streamer at the designated depth.

Data acquisition systems

Data were recorded with acquisition software provided by Geometrics. The analogue signal was digitized with 4 kHz. The data were recorded as multiplexed SEG-D. One file was generated per shot. The acquisition PC allowed online quality control by displaying shot gathers, a noise window, and the frequency spectrum of each shot. The cycle time of the shots is displayed as

well. The software also allows online NMO-Correction and stacking of data for displaying stacked sections. Several logfiles list parameters such as shot time and shot position. Data were converted to SEG-Y file while being at sea.

Trigger unit
A long shot was used as gun controller. The Injector was triggered with a delay of 10 ms. The arming point for the gun was set to 60 ms or 80ms. Due to problems with the hydrophones at the gun, no direct quality control of the source signal was carried out.

5.2.3. First results of 2D seismic survey

Preliminary data processing was carried out for all profiles onboard. Several channels of each shot were filtered and stacked. These brute stacked were loaded to a seismic interpretation system (HIS Kingdom Suite) and used for preliminary interpretation. In total we collected about 740 nm of seismic 2D miles of seismic profiles off Southern Italy (see Fig. 2).

The first survey area was the Gioia Basin (Fig. 11). The basin is dominated by the Gioia-Messima canyon-channel system (Gamberi and Marani, 2008). The Gioia-Messima canyon-channel system is the biggest tributary of the Stromboli Canyon, which crosses the basin longitudinally and cuts deeply into the bottom in front of the Panarea and Stromboli volcano. An example of a profile crossing the Gioia-Messima canyon-channel system is shown on Fig. 12. Two canyons are deeply incised in the background sediments. Incision depth for Gioia and Messina Canyons are 75 m and 45 m, respectively. No obvious faults are found beneath the canyon thalwegs. Messima canyon shows a left-hand levee, which is probably the result of flow stripping in an outer meander bend. No levees are imaged for Gioia Canyon. The incision depth might be too large for significant overspill of turbidity currents. No obvious sedimentary fill is found for both canyons indicating that they are active sediment transport pathways. The sedimentary succession can be divided in three different units. The upper most Unit 1 is about 100 ms TWT thick; it is characterized by high amplitude reflectors of medium continuity. The canyons are incised in this unit. Unit 2 shows slightly reduced amplitudes but much better continuity. The reflectors are more or less horizontal. Unit 2 and 3 are separated by an unconformity (onlap of Unit 2 on Unit 3). The reflectors of Unit 3 are inclined and slightly folded. Some mass transport deposits are imaged in the surface.

A dense net of seismic lines were collected in the inner Messina Straits (Figs 13, 14). The main aim was to investigate fault patterns in this region. Due to great support of Messina Traffic Control (Messina VTS) it was possible to run straight profiles through the traffic separation area resulting in a unique dense net of seismic profiles in this area. Some problems occurred with fishing lines caught by the streamer.

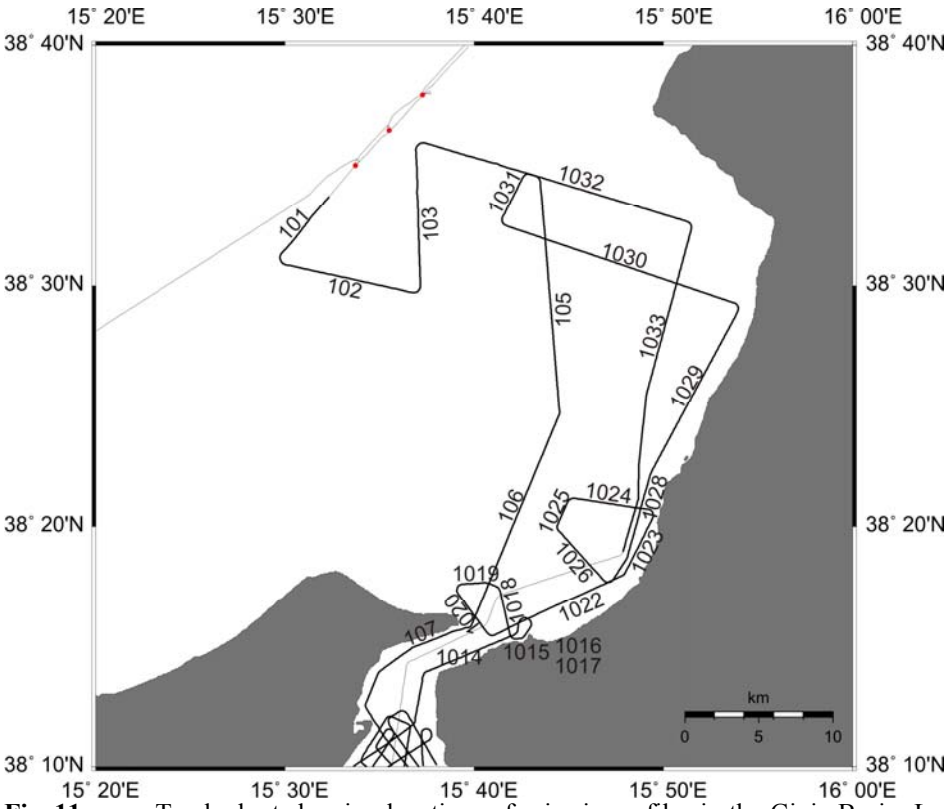

Fig. 11 Track chart showing locations of seismic profiles in the Gioia-Basin. Location of cores are shown in red.

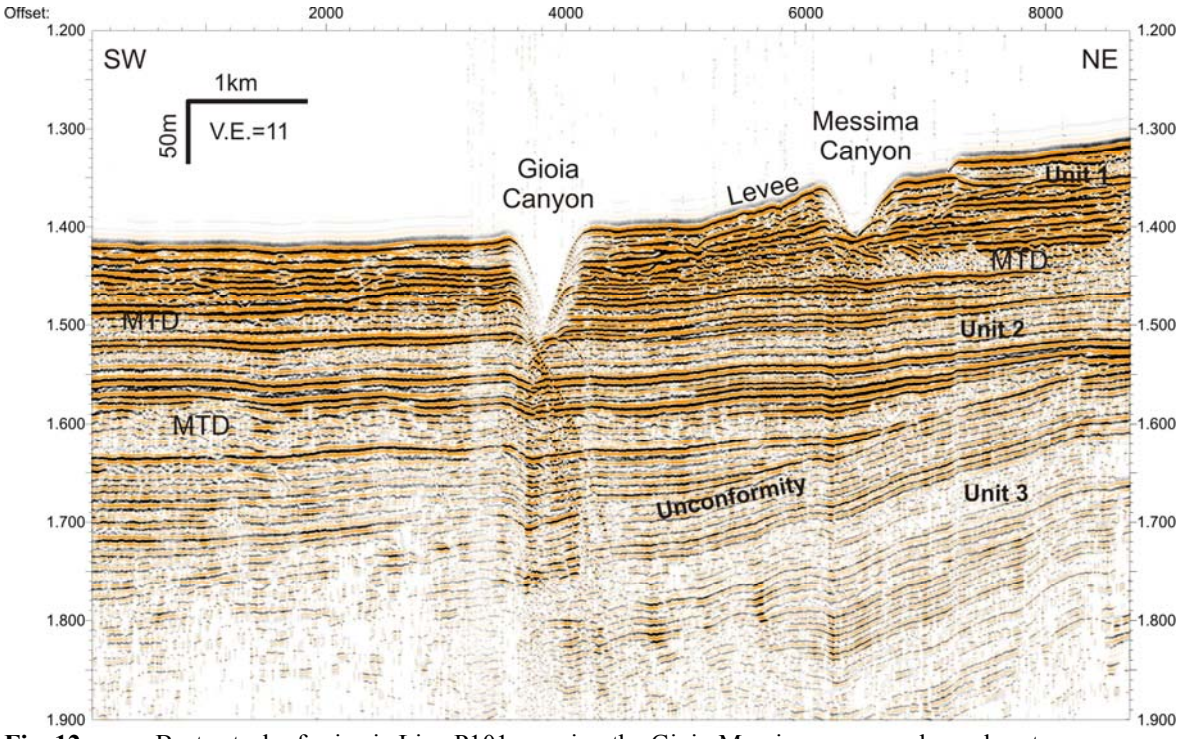

Fig. 12 Brute stack of seismic Line P101 crossing the Gioia-Messima canyon-channel system. Location of profile is shown on Fig. 11.

One example crossing the Messina Straits is shown on Fig. 15. This profiles show a complex pattern of unconformities on the NW Sicilian side. The Messina Canyon is incised in sediments in the central part of the profile. Several tributary canyons are found at the SE Calabrian side of the profile. A central objective of the survey in the Messina Straits is the identification of

possible seismogenic faults. Several faults are visible on the profile. E.g., the location of the Messina canyons seems to be controlled by faults. Several of the faults can be traced using the dense net of seismic profiles. They seem to run in a N-S direction more or less parallel to the axis of the Messina Canyon. However, only some of the faults reach the surface. The close net of seismic profiles will allow studying the activity of the faults in detail, which is essential in order to assess their seismogenic potential.

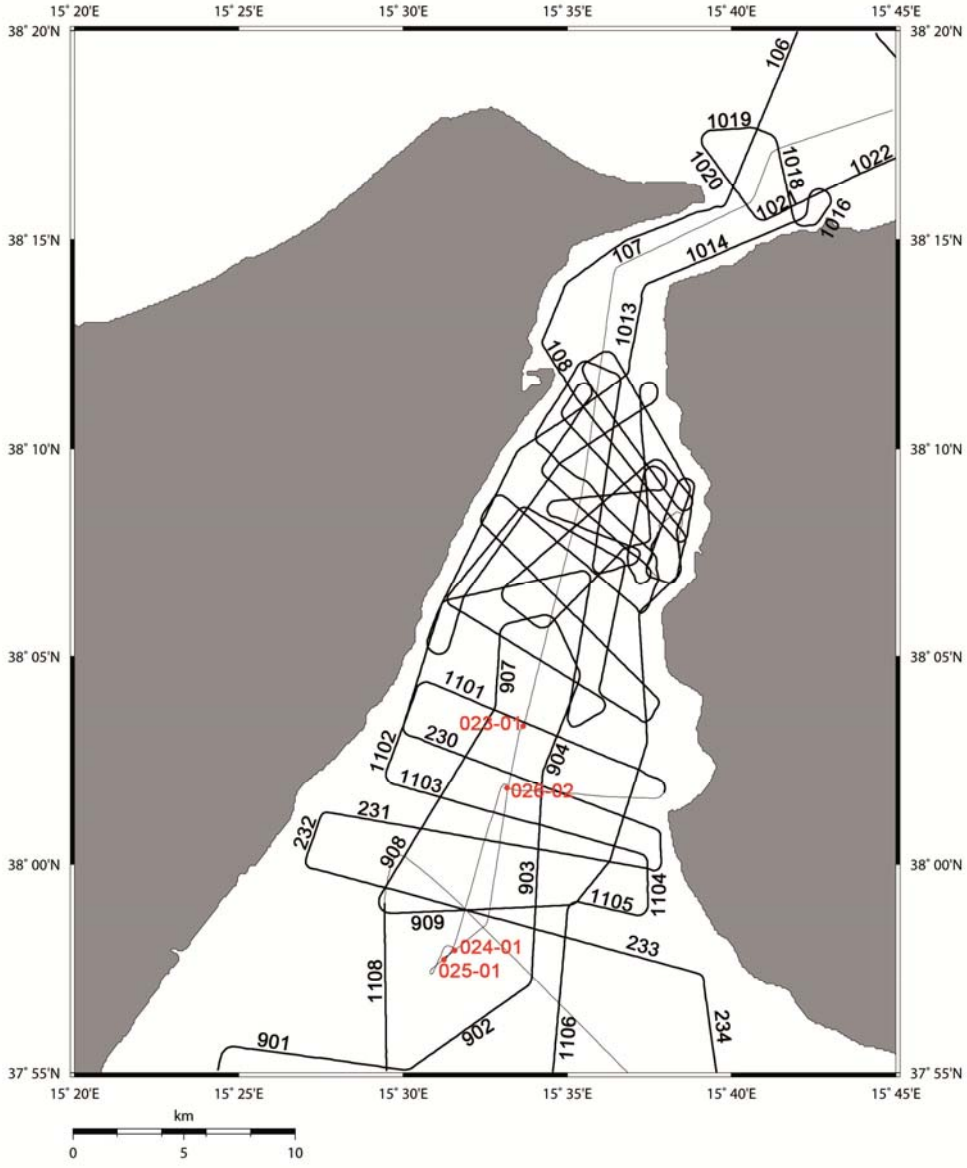

Fig. 14 Track chart of seismic profiles collected in the inner Messina Straits. Location of cores are shown in red.

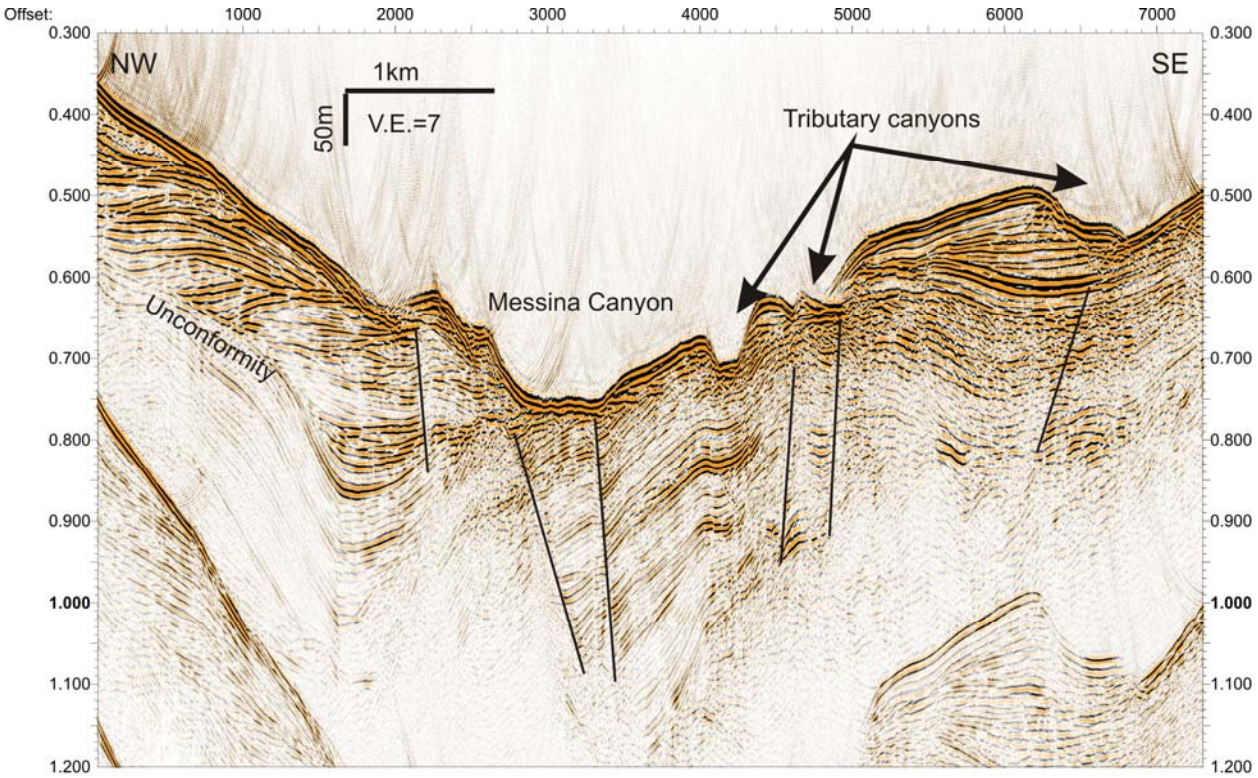

Fig. 15 Migrated seismic profile P215 crossing the Messina Straits. Possible faults are marked as thin black lines. See Fig. 14 for location of profile.

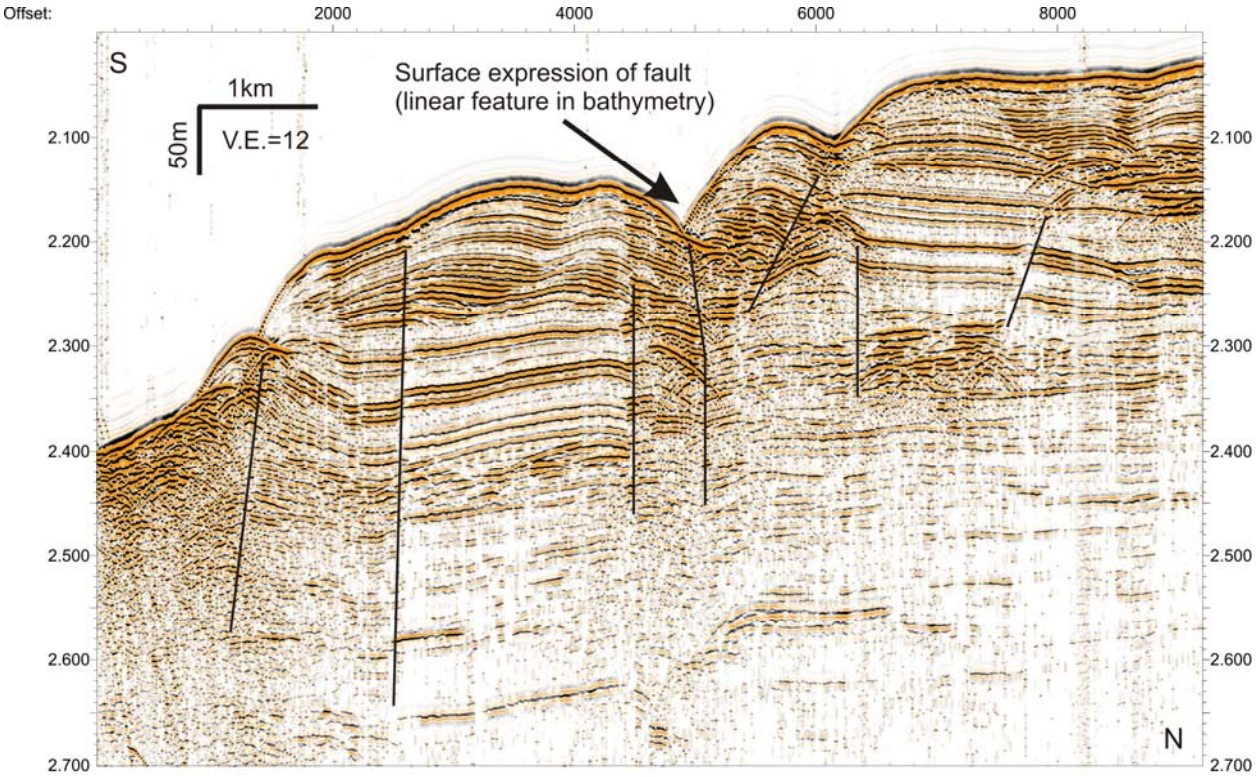

Fig. 16 Brute stack of Profile P805 crossing a linear feature identified in the bathymetric data. See Fig. 17 for location of profile.

A very prominent linear sea floor feature can be identified on the bathymetric map of the outer Messina Straits (see Fig. 4 for location). Profile P805 crosses the central part of this feature (Fig. 16). The profile shows numerous fault. A normal fault reaching to the surface is clearly visible in the central part of the profile. The same observation is made for all profiles crossing the linear feature identified in the bathymetry. Hence this feature is the surface expression of a fault. This fault is very close to the location, where Billi et al. (2008) identified the most probable tsunami source area for the 1908 Messina tsunami. Hence this fault may have played an important role during this event. The fault runs in an E-W direction which is almost perpendicular to the strike direction of all previously postulated faults. Future work need to investigate how this observation fits to the general geodynamic setting of this area.

A dense net of seismic profiles was also collected east of Sicily (Fig. 17). The 3D-seismic data set is also located in this area (see chapter 5.3.). An example of a 2d-seismic line is shown on Fig. 18. This profile crosses an area, where Billi et al. (2008) postulated a large slide, which may have triggered the 1908 tsunami. The profile crosses several deeply incised canyons and show clear mass transport deposits. These deposits are covered by a thick succession of undisturbed and stratified sediments. Hence they are old deposits which clearly show that the area is general prone to slope failure. However, no young slide deposits are identified in this area.

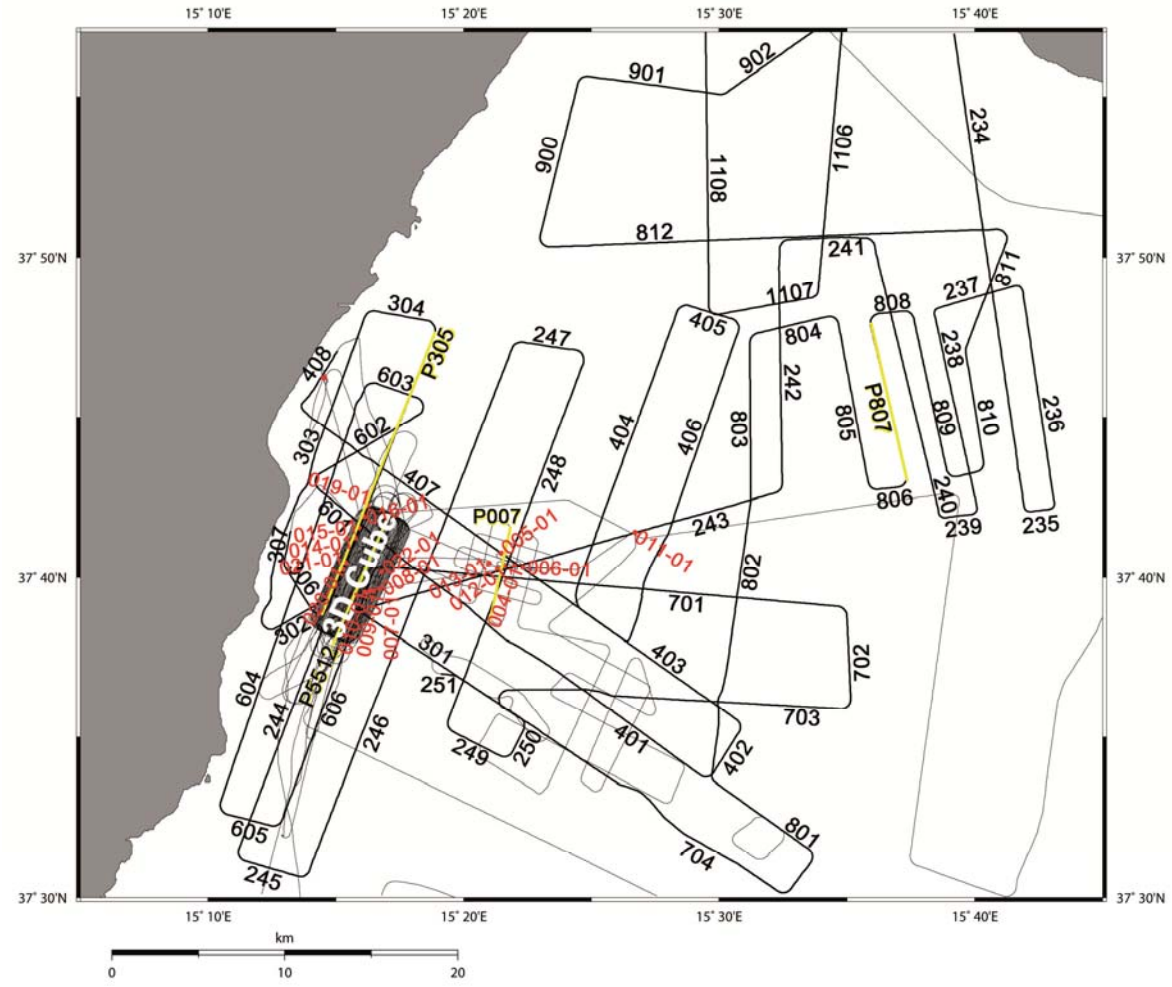

Fig. 17 Track chart of seismic profiles collected east of Sicily. The yellow lines represent the Parasound profiles (P007, P305, P807, P5512) described in chapter 5.1.2. Location of cores are shown in red.

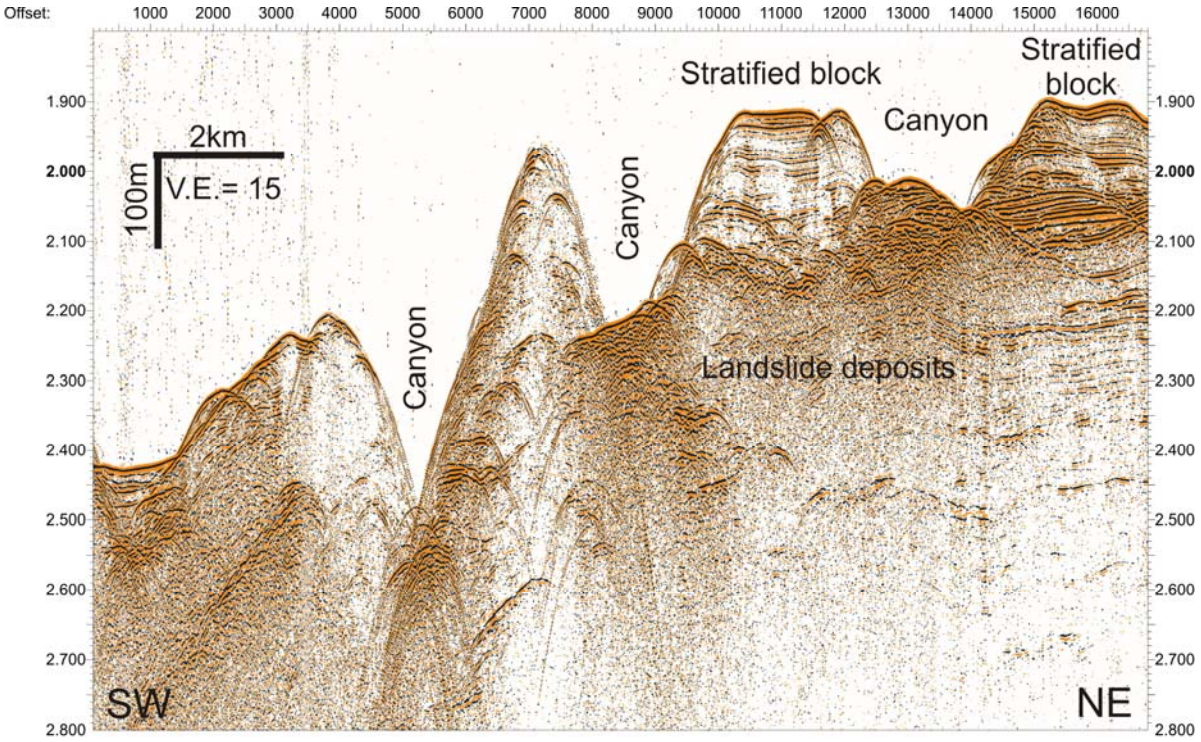

Fig. 18 Brute stack of seismic profile P404 east of Sicily. See Fig. 17 for location of profile.

5.3. P-Cable Multichannel 3d Acquisition

(J. Bialas, C. Papenberg, G. Crutchley, S. Koch, T. Matthiessen, G. Wetzel)

5.3.1. P-Cable Streamer System

The P-Cable (VBPR patent of 2003) system design is similar to the SwathSeis idea, which was investigated by theoretical modelling funded through the DFG by IFM-GEOMAR in 2001/2002. Basic idea of both systems is the three dimensional seismic imaging of the oceanic crust. While SwathSeis is dedicated to basement mapping the P-Cable design is oriented to high resolution of shallow horizons. GEOMAR is holding an academic license of the P-Cable system covering development and application of such a system.

Compared to standard reflection seismic applications in 2-D and 3-D the basic difference is that the P-Cable is built by a cross cable towed perpendicular to the ships heading. Instead of a few single streamers the P-Cable uses a large number of short streamer sections towed parallel from the cross cable. Drawback is the limited depth penetration due to the short offsets, which do not allow the removal of the multiple energy. This is well compensated by the reduced costs of the system and the ability to operate it even from small multipurpose vessels, the usual academic platform for marine research. Cruise M86/2 was the first deployment of the P-cable on RV Meteor.

Fig. 19 shows the basic principle of the P-Cable design. The advantages of the GEOMAR development are twofold. The cross cable is based on a strength member, a Dynema rope, which takes the stretch forces of the trawl doors (Fig. 20). Attached to this rope is the data cable with the streamer connections (Fig. 21). GEOMAR developed a modular cross cable, which allows exchange of each single streamer connector (node) with data cable and strength member section in case of a malfunction. This allows easy service and reduced service costs. Other systems were built by a data cable molded in one piece, which need to be replaced as whole part if one node

fails. In addition the modular design allows to insert connecting cables of different length between the nodes. Hence an adoption to different resolutions of P-Cable and SwathSeis application is possible. The current grade of the system provides 13 active nodes connected by 15 m and 10 m long data cables. On both sides the closest node is located 11.7 m off the triple point. The 165 m long cross cable is stretched by two trawl doors, floating at the sea surface. Floats attached to each break out help to keep the streamers at 2 m depth (Fig. 22). Each one of the trawl doors provides a lifting force of 2 tons. Although the doors are designed to provide maximum lift at 4 kn sailing speed the cross cable was stretched to about 130 m width at 3.3 kn already.

On board R/V METEOR the trawl doors were located on the working deck next to the aft A-frame (Fig. 23). Upon deployment the door next to the umbilical is released from its rest position (Fig. 24) while the ship sails at 1 kn through water against wind and waves. The door is lowered into the water while a 10 m long lead cable between door and connection point of cross cable is kept on board. Next the data cable from the recording device to the door is hooked to the connection between lead wire and cross cable. Now trawl wire, data cable and cross cable are payed out simultaneously (Fig. 25). At the same time streamer sections are connected to the nodes of the cross cable. Floats are fixed to each node in order to keep the cross cable at even depth (Fig. 23). When the entire cross cable is paved out a 50 m support rope on the support winch is used for secure transfer of the cross cable from the support winch to the lead wire of the second trawl door (Fig. 24). Now both trawl wires are given out until the final length with sufficient stretch of the trawl doors is reached (Fig. 24, 25)

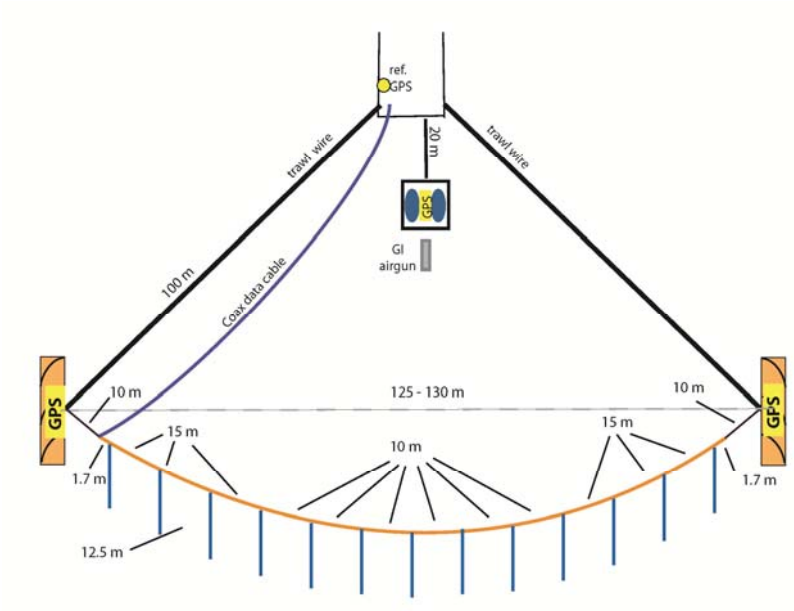

Fig. 19 Sketch of the P-Cable design applied during the M86-2 cruise.

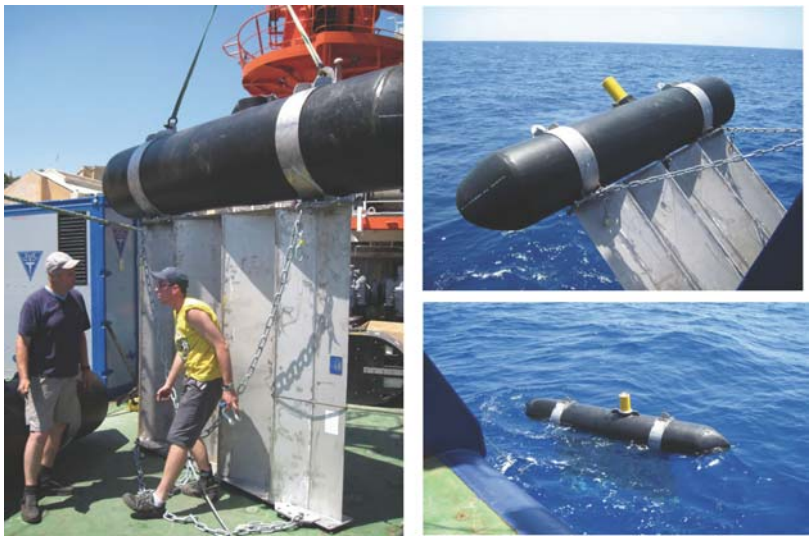

Fig. 20 Photographs of the trawl doors. Left: floats are mounted on the paravanes. Top right: half way lowered, ready for deployment. The yellow cylinder houses the GPS receiver and the radio modem. Bottom right: floating away from the vessel.

Fig. 21 Photograph of cross cable, drop leads and streamer section during dry test on board.

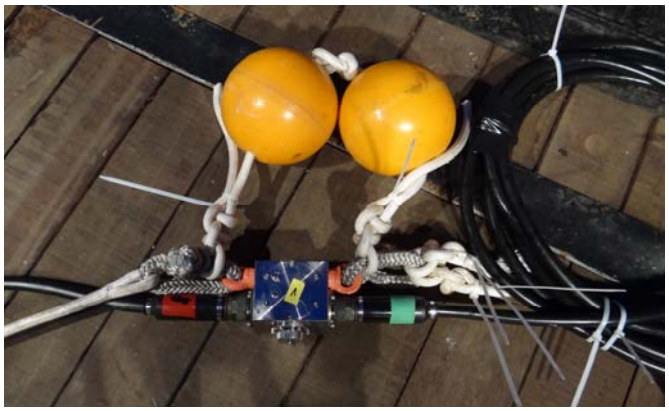

Fig. 22 Floats are fixed on the cross cable in order to keep it at about 2 m depth during profiling.

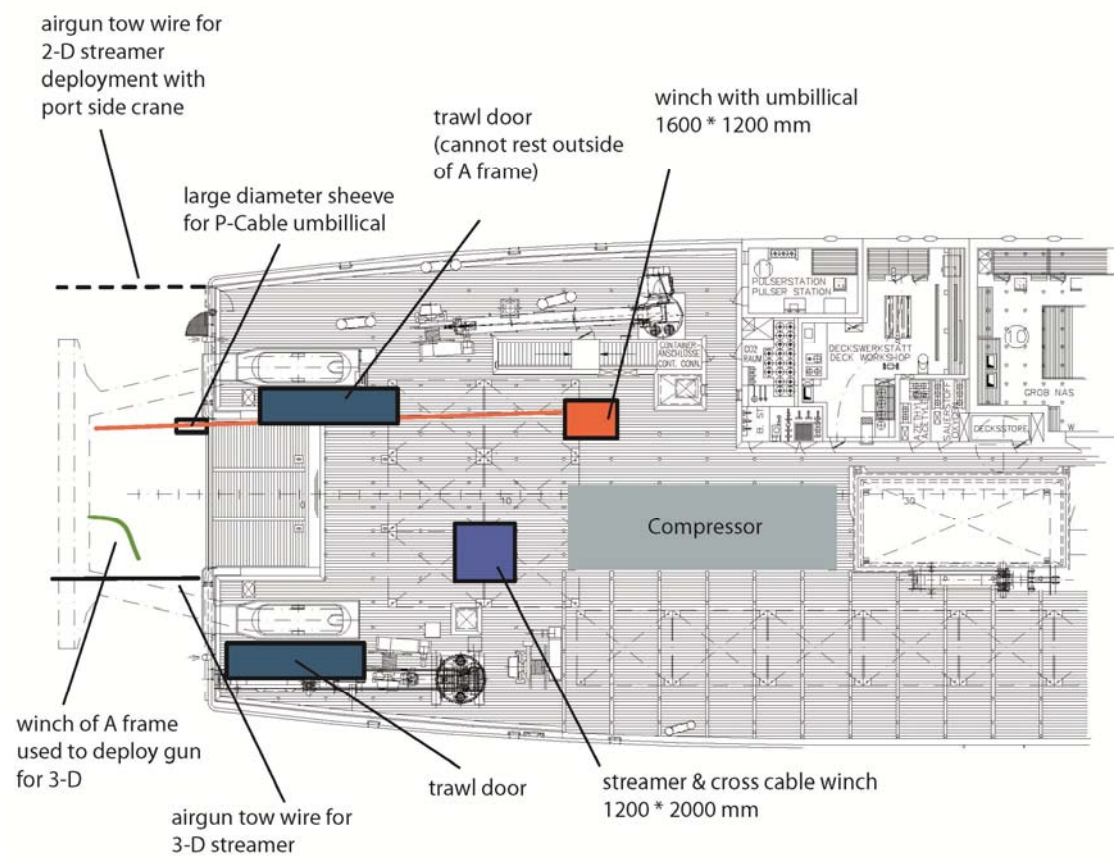

Fig. 23 Distribution of the seismic equipment on the aft deck of R/V METEOR during cruise M86-2.

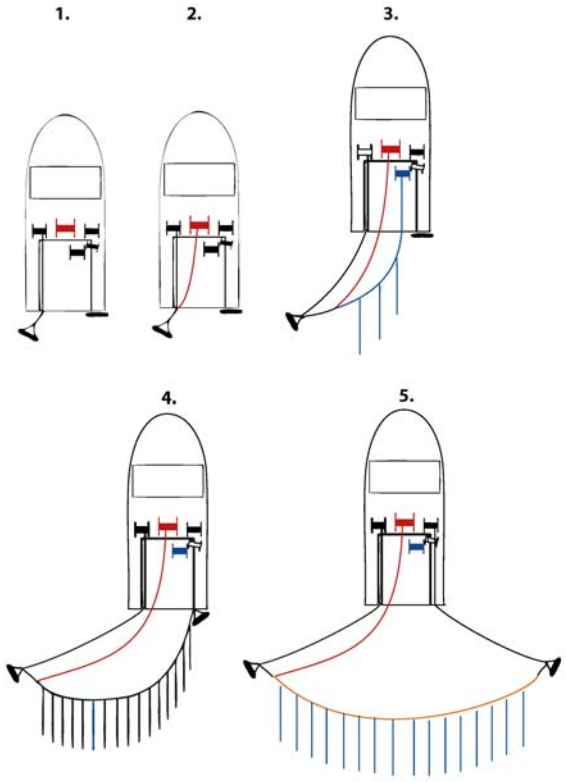

Fig. 24 Sketch illustrating the steps during deployment. See text for details.

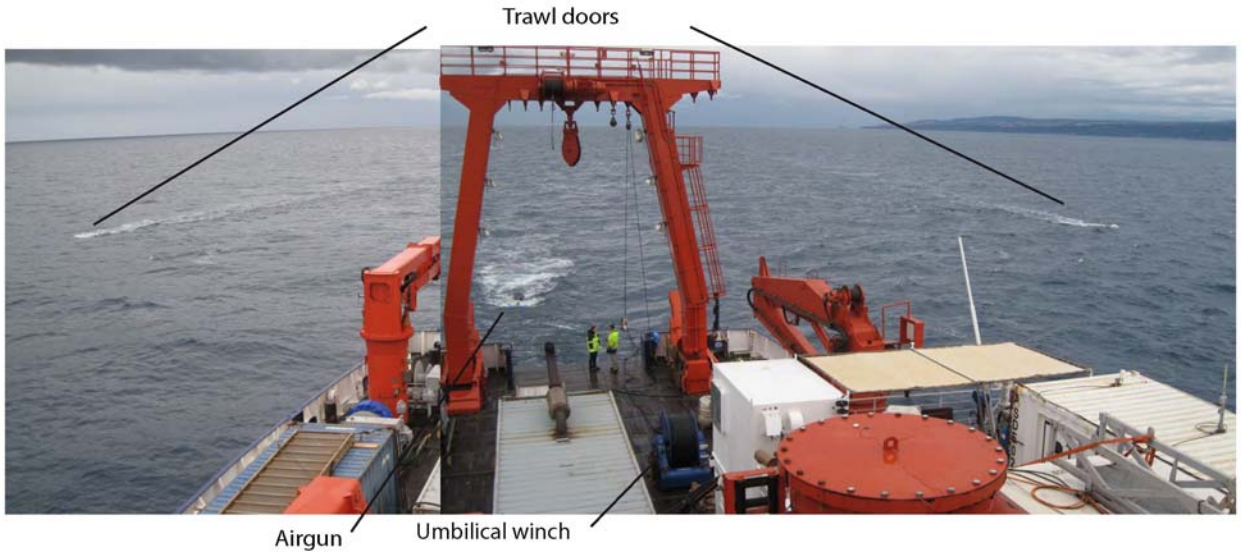

Fig. 25 Photograph of the towed equipment with indication of system parts.

5.3.2. Navigation processing

Several Ashtec AC12 GPS receivers were set up to provide position information of the various systems. On board a GPS antenna was mounted on the port side next to the stern of the ship (Fig. 26). Additional GPS receivers were mounted on the two trawl doors and the airgun for the 3-D P-Cable system. NMEA strings from the remote GPS were transmitted via radio link on board R/V METEOR. RS232 links submitted the position information to the navigation PC. All GPS data were recorded and stored via Telnet port reader. A custom software reads the strings and provides network wide distribution via TCP/IP port access. Program OFOP was used to display

the ships and trawl doors positions on top of a bathymetric map. Track keeping accuracy could be controlled by the display of the waypoints. In addition offsets between trawl doors and trawl door – ship were displayed. The OFOP laptop in the seismic lab did broadcast the GPS information of ship, trawl doors and gun in the ships network. From here it is possible to run OFOP on other machines with the same GPS display possibilities. If one of such PCs allows a VNC screen copy it is possible to have a copy of a dedicated screen displayed on the bridge.

With the P-Cable system the streamer sections are not distributed along a straight line. Due to drag forces in the water the cross cable can best be described forming a shape somewhere between a triangular and a half circle. Navigation processing aims in calculating the exact shape by using the GPS positions of the trawl doors and the first arrival time of the direct wave from the airgun signal. During the course of profiling the trawl doors were affected by water currents and sea state. Therefore offsets between starboard and port side door and the airgun in the center are varying depending on the heading of the sail line. Based on GPS positions of the trawl doors and the first arrival of the airgun shots at the streamer hydrophones the position of each streamer segment is calculated (Fig. 27). Triangulation is applied and provides coordinates for the streamer groups within a range of less than 5 m. The assumption of a catenary shaped outline for the cross cable provides best results. Based on the resulting shot table coverage, interpolation, stacking and migration of the entire data cube can be done. The navigation routines and coverage calculations were routinely calculated by endless looping shell scripts. Hence every 15 minutes an update for the achieved coverage is available (Fig. 28). For the raw processing on board R/V METEOR a migration grid of 6.25 m * 6.25 m could be achieved.

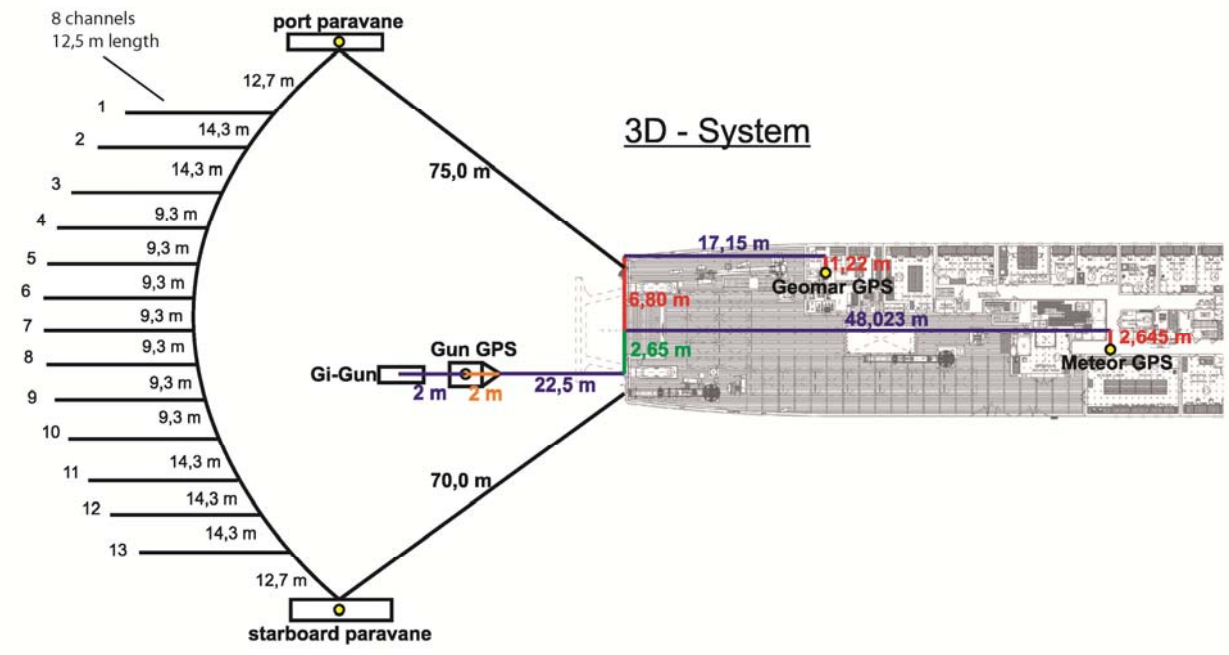

Fig. 26 Working deck of R/V METEOR with offsets for antennas and towed equipment.

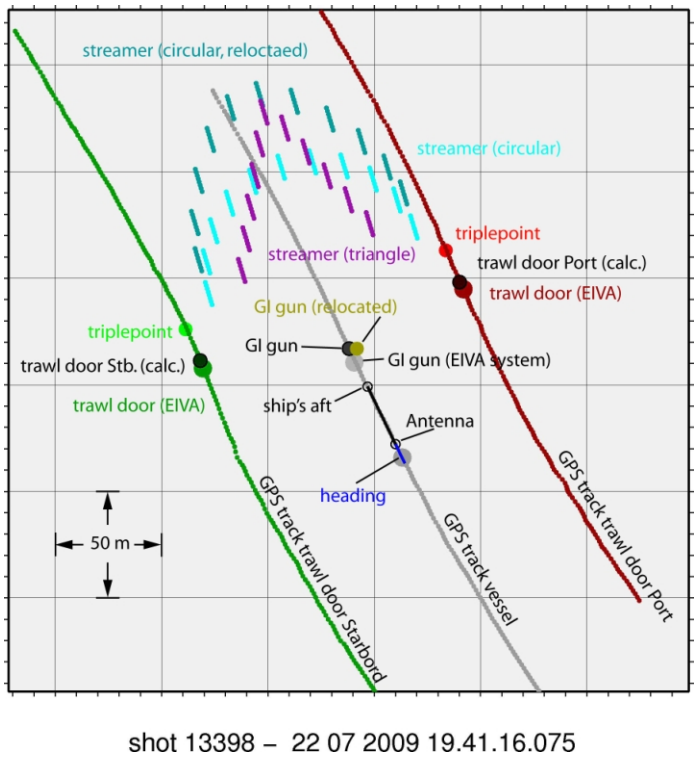

Fig. 27 Plot of the navigation information used for each shot to calculate the streamer positions. All relevant coordinates (GPS, calculated) used during the calculation of the best fit streamer distribution are plotted and named. Misfit control of first arrival times on hydrophone no. 1 in each streamer is used as confirmation for the correct geometry.

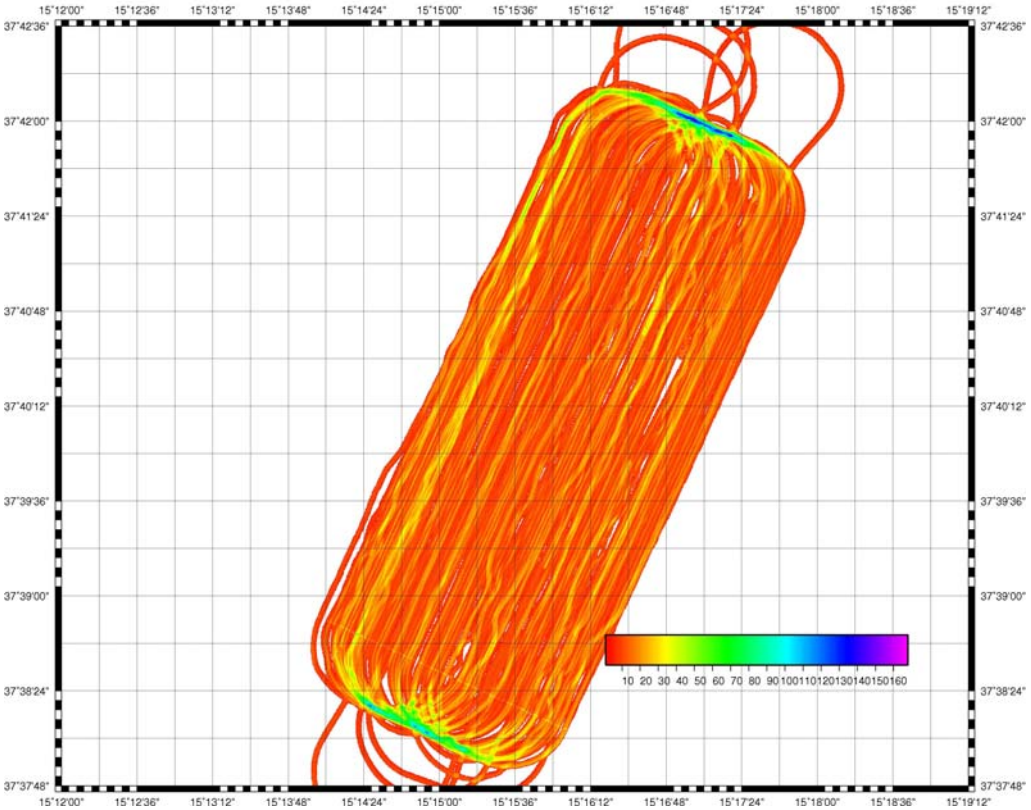

Fig. 28 Coverage map short before the 3D acquisition was terminated. The color scale shows the fold in each bin of the 3D area. Due to multiple coverage the coverage in the turns is highest. Bin without coverage are left white. Undulations along the sides of white stripes indicate deviations from the track line during data acquisition.

5.3.3. Fieldwork

For the 3D cube an area of 4.2 nm * 1.7 nm was chosen at the foot of the Etna volcano (Fig. 29). The sea floor morphology shows major lineaments, which are indicating possible faults and fractures that show a high variation in strike.

To the NE of the 3D survey area NE-SW striking lineaments at the seafloor are of major scientific interest. Three major theories are discussed as cause for the fissures. One assumption is that they are the seafloor expression of slump planes, along which the slope collapses. To the East of the 3D cube a major circular depression would represent the frontal end of seafloor failure. A second hypothesis suggests that fluid migration from below stimulates chemical and biologic activities that result in seafloor compaction and ridge formation. Both scenarios imply that subsurface processes are the cause for this extinct seafloor morphology. A third explanation assumes that elongated geologic bodies "float" on the slope sediments. With the dense 3D seismic imaging we intend to reveal the subsurface structure beneath these structures and want to contribute to the pro and contra of the discussion.

The central part of the 3D data cube covers the funnel shaped outflow region of the Zavianne River. Deep cutting grabens separate two ridges against the continental slope to the North. The change of 45° in strike between these graben structures and the above described fissures indicate that they belong to a different tectonic structure. The picture becomes even more complex with the continuation further south. Here at the limit of our 3D survey exposed ridges are dominating the seafloor morphology. Contrary to the northern limit of the delta outflow area the strike of the Southern lineaments is SW-NE, more or less perpendicular to their northern opponents. Although the southern features are at the limit of the cube we hope to image their depth continuation with sufficient precision to gain further understanding of the related tectonics.

In total we collected 90 sail lines and fired 116328 shots in the 3D-box. A first migration along inline and crossline direction could be completed three days after termination of the data acquisition. The data were binned at 6.25 m bin-size in inline and across-line direction. The correlation of the seafloor between inlines and crosslines confirmed already a very precise navigation processing, which is the most important component for a precise image. First displays of the inlines revealed the complex geometry of the sediments (Fig. 30). Well stratified regions interplay with transparent or chaotic reflection patterns. Notable vertical offsets observed already in the bathymetry continue as fault in the subsurface. In addition elder, covered faults exist, which may not be active today. The chair cut image through the data volume (Fig. 31) highlights the interpretative possibilities provided by the data set. Faults and sedimentary sequences may not only be referenced at a single position but can be described in their entire distribution. Strike direction and slope angles can be calculated. Faults can be identified and followed along their distribution in the volume.

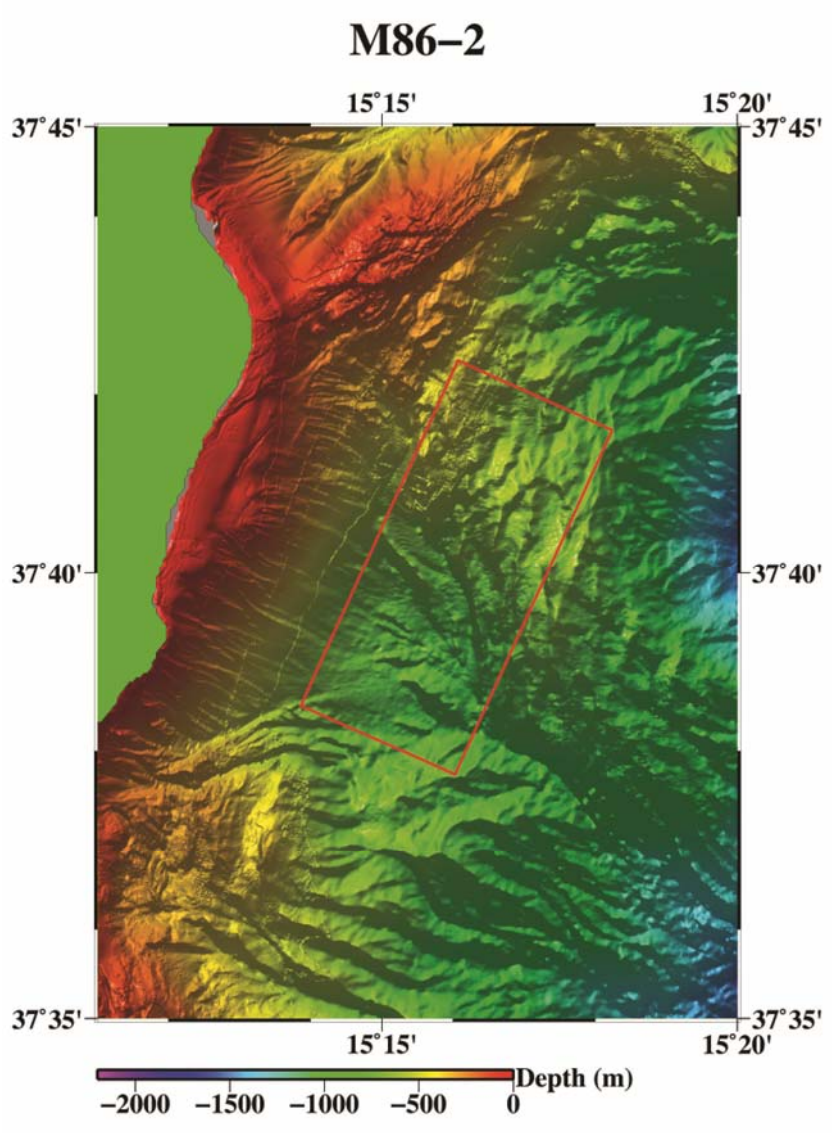

Fig. 29 Bathymetric map showing the location of the 3D-cube.

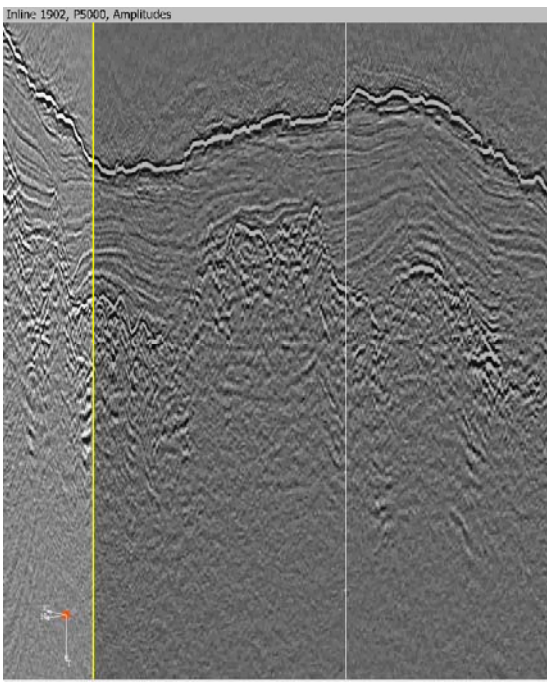

Fig. 30 xample of an inline revealing the complex geometry of the survey area.

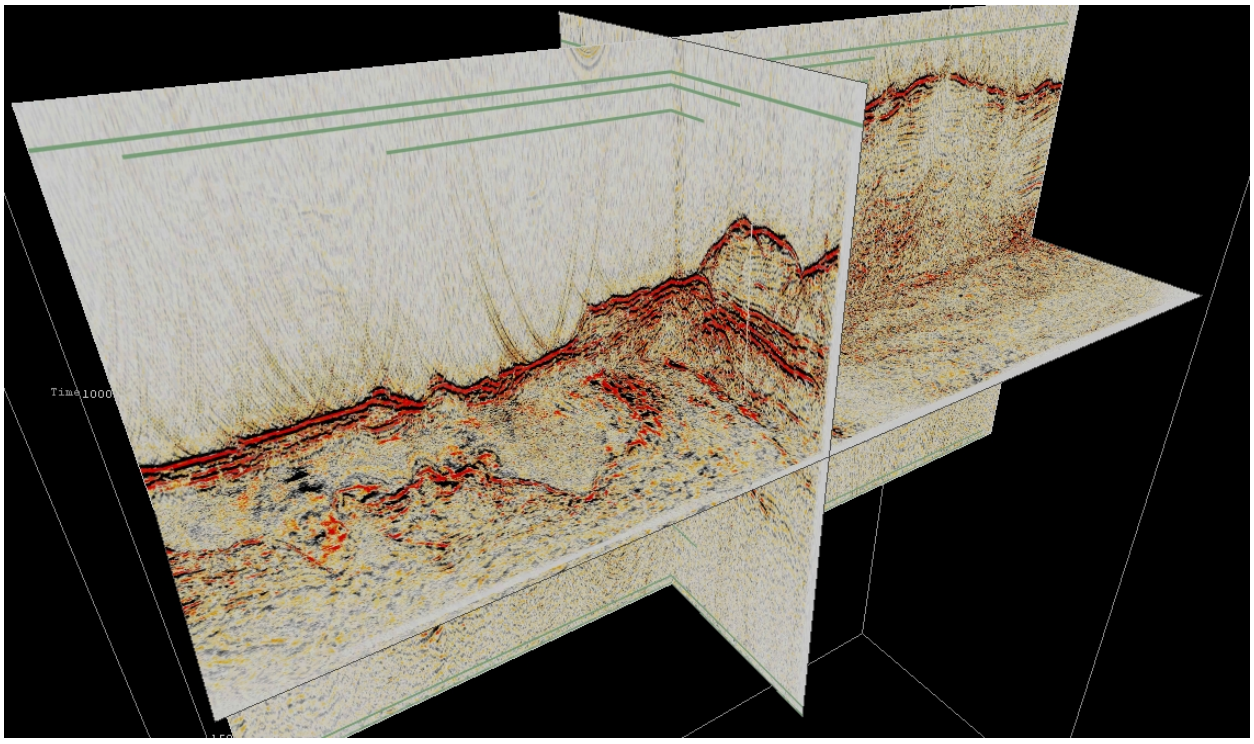

Fig. 31 Example of a chair cut image of the 3D-cube.

5.4. OBS Deployment

(J. Bialas, C. Papenberg, S. Koch)

Due to the limited active length of the applied streamer systems the shot records will not be sensible for a variation of sound velocity with penetration depth of the reflected signals. As such information would be significant additional information to the structural images provided by the MCS sections, four Ocean Bottom Seismometers (OBS) were deployed within the 3D coverage area (Fig. 32, Tab. 4). The OBS recorded all shots from the 3D survey and hence will provide wide angle reflection and refraction information up to 8 km offset. The four deployment positions were chosen according to the expected major geological formations within the area of investigation. 1D velocity depth profiles derived from the OBS observations should further support to distinguish between separate geological units.

Technical Description

The GEOMAR Ocean Bottom Seismometer 2002 (OBS-2002, Figure 33) is a design based on experiences gained with the IFM-GEOMAR Ocean Bottom Hydrophone (OBH; Flueh and Bialas, 1996) and the IFM-GEOMAR Ocean Bottom Seismometer (OBS, Bialas and Flueh, 1999).

Four main floatation cylinders are fixed within the system frame, while additional disks can be added to the sides without changes. The basic system is designed to carry a hydrophone and a small seismometer for higher frequency active seismic profiling. The sensitive seismometer is deployed between the anchor and the OBS frame, which allows good coupling with the sea floor. The three-component seismometer (*KUM*) is housed in a titanium case, modified from a package built by Tim Owen (Cambridge) earlier. Geophones of 4.5 Hz natural frequency were used.

While deployed to the seafloor the entire system rests horizontally on the anchor frame. After releasing its anchor weight the instrument turns 90° into the vertical and ascends to the surface

with the floatation on top. This ensures a maximally reduced system height and water current sensibility at the ground (during measurement). On the other hand the sensors are well protected against damage during recovery and the transponder is kept under water, allowing permanent ranging, while the instrument floats at the surface.

The signals of the sensors are recorded by use of the *Marine Broadband Seismic Recorder (MBS)* manufactured by *SEND GmbH*. The MBS-Recorders are specially designed for short-time high-resolution recordings due to their high precision internal clock. For our purpose we run the MBS-Recorder with 1000 Hz sampling frequency. Clock synchronization before deployment and drift check after recovery are compared to GPS time. The samples are saved on PCMCIA storage cards together with timing information. After recovery the data stored on up to four flash cards are combined into one data set and formatted according to the PASSCAL data scheme.

Data recorded

All four OBS worked well during the entire data acquisition time within the area of the 3D cube. Fortunately the instruments were deployed the night before the 3D acquisition started. Therefore the systems could already monitor micro-seismicity events emitted from the Etna eruption, which happened during the morning of 5th Jan. 2012 (Fig. 34). Although the Eigenfrequency of the OBS sensors were not designed for seismological observations three significant events are visible prior to the start of the active seismic profiling. The third event happened at 04:30 local time, when lava eruptions could be observed by the ship's crew. The two predecessor events seem to indicate precursor events of the Etna. They may be caused by migration of Lava in the volcano.

Fig. 35 shows an inline observation of OBS 503 during active seismic profiling. Clearly visible are the first arrival and the later multiple arrival. The OBS was located next to shot point 29450 where the shortest travel times are recorded. Although no data processing has been applied to the section numerous reflection events can be identified in the time window of 0.6 sec to 1.1 sec at shot point 29450. With the wide angle observations of up to 3 km a one dimensional velocity depth model can be calculated. Further information about geological units within the 3D area can be deduced by comparison with v-z distributions of the other three instruments.

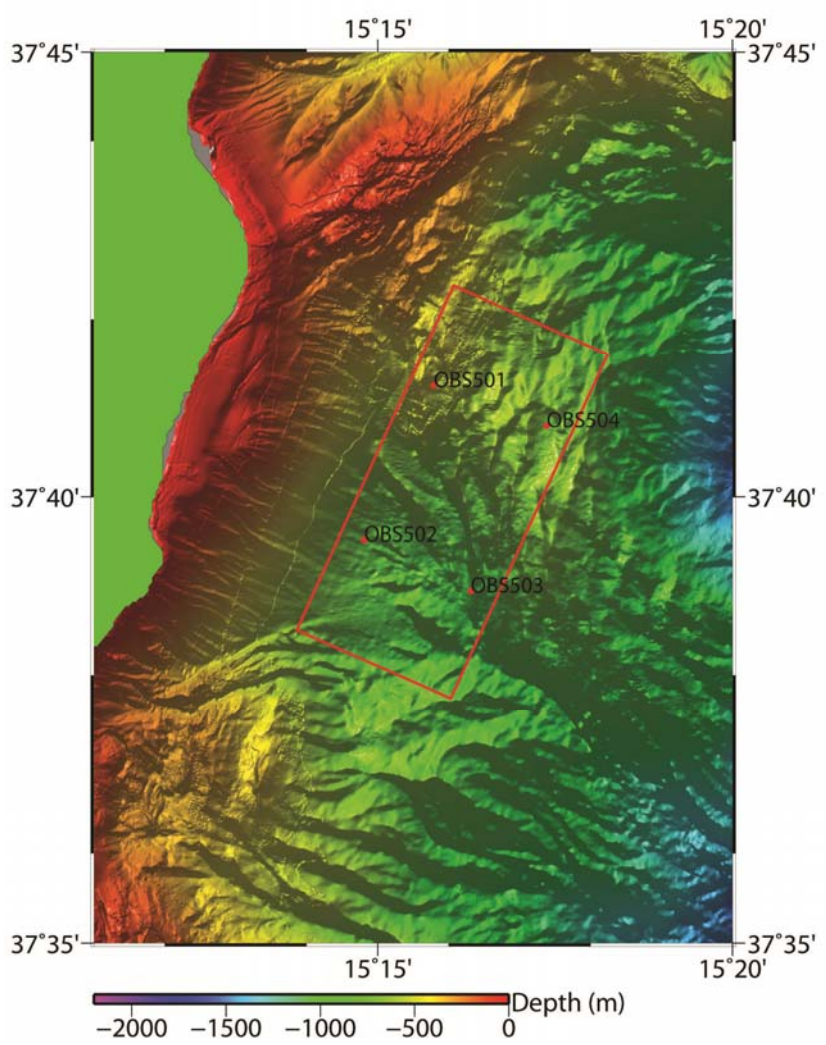

Fig. 32 Map of the OBS deployment. The 3D area is indicated by the red colored boundaries. The deployment positions of the four OBS are indicated by red dots. Positions have been chosen according to the expected major geological structures forming the area of investigation.

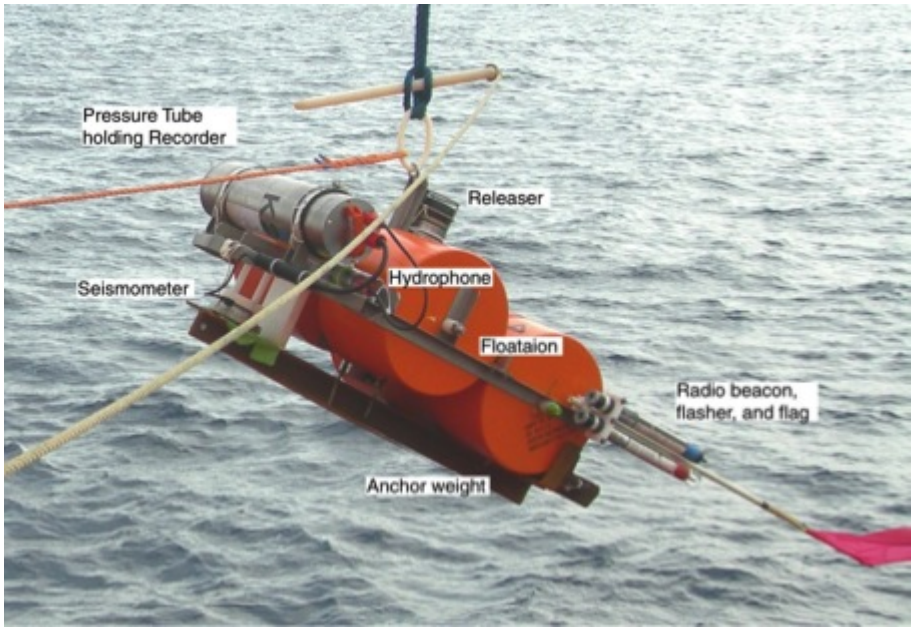

Fig. 33 The IFM-GEOMAR Ocean Bottom Seismometer design 2002 upon deployment

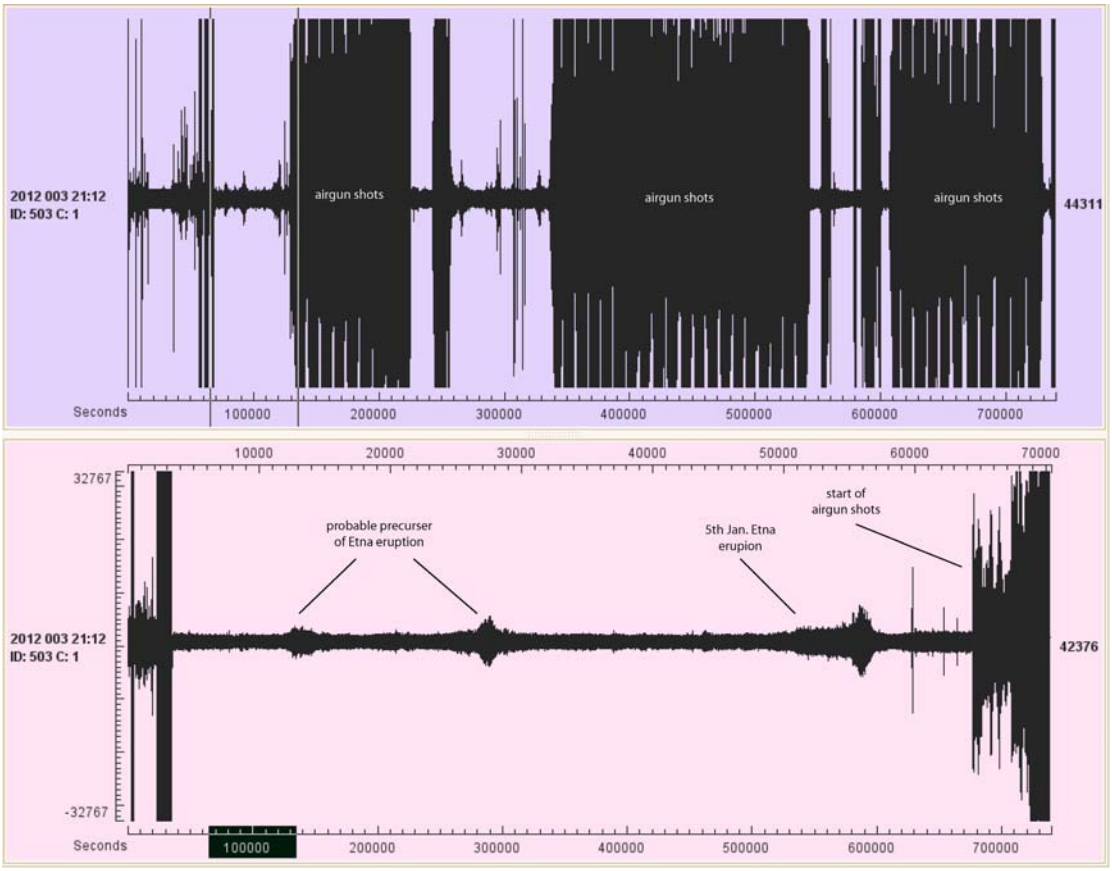

Fig. 34 Overview display of the hydrophone records taken from OBS 503. Top: Display of the entire data stream which was continuously recorded during the deployment. Bottom: Enlargement of the first 2 hours of recording. The left hand large amplitudes are due to deck handling and descending to the seafloor. The three smaller events at 15000, 20000 and 58000 sec. seem to be caused by the Etna eruption.

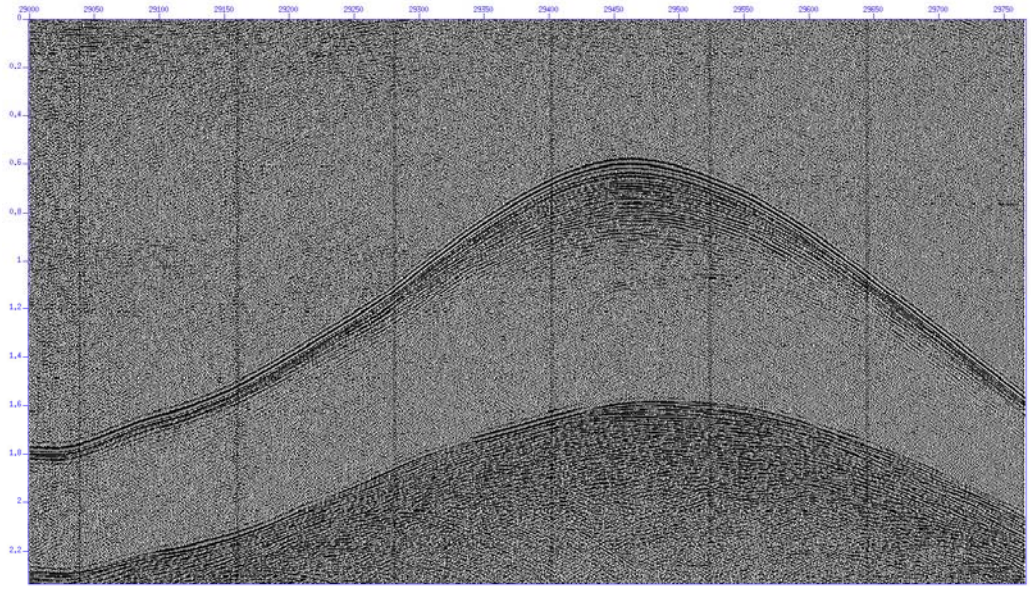

Fig. 35 Inline observation of OBS503 during the active seismic profiling. First arrival and the multiple reflection are clearly visible. Numerous reflection events are already visible following the first arrival in this raw data section.

5.5. Sediment Sampling

5.5.1. Introduction

(D. Winkelmann, J. Schwab, M. Urlaub, F. Groß, J. Beier)

During cruise M86/2, gravity cores were mainly taken in order to sample landslide deposits and ridges and their direct vicinity in the seismic 3D-cube. We used a standard gravity corer and a giant box corer at selected stations. A station list is given in the appendix (Tab. 3). The core locations are shown together with seismic lines on Figs. 11, 13, 14, 17.

The Giant Box Corer (GBC) was used in areas, where we expected coarse-grained surface covers. This was the case in the Messina Canyon and at a possible mud volcano site close to the shore. The Giant Box Corer was applied at 4 stations (Tab. 3). The over-standing water was removed after retrieval and the sediment surface was described and photographed. Then, the front wall was opened and the downcore profile was described and photographed. Finally, surface and downcore-profile samples were taken.

A standard gravity corer was the main tool for sediment sampling. The top weight was 1.5 tons. After retrieval, the core liners were cut into 1-m long sections, closed with caps and labeled according to the general GEOMAR scheme. Selected cores were cut down-core into two halves: one containing the *Work* and the other the *Archive* material. Due to time constraints, only a few selected cores were opened onboard. All other cores were opened quickly after the cruise in the labs of GEOMAR.

During the cruise, 26 sediment cores from 25 stations were recovered using a Gravity Corer (GC) with station-individual lengths of 6 or 12, respectively (Tab. 3). Total core recovery was about 80m.

5.5.2. Coring strategy

A set of three cores were taken across a landslide scarp in the Gioia Basin (M86/2-1 – 3, see Fig. 11 for location of cores). One core was taken immediately above the landslide scarp in undisturbed deposits while two cores targeted the landslide deposits itself. Landslide deposits are easily identified in these cores, which seems to be covered by 160 cm thick, undisturbed sediments (e.g. Core M86/2-007-01, see Fig. 36).

Most cores were taken off Eastern Sicily. A set of cores (M86/2-004-006, 012, 013, see Fig. 17 for location) were taken in a small basin beneath a major amphitheater-like scar (see Fig. 4). Parasound data show stacked mass transport deposits in this basin (see Fig. 5). Another core was taken close to this basin in a canyon thalweg (M862-11). All of these cores show abundant mass transport deposits.

Several cores were taken in the area of the 3D-cube. Cores M862- 7 – 10, 20 -22) were taken on or next to ridges identified in the 3D-cube. Several hypotheses are available for the generation of these ridges. They may represent deformation patterns, rafted blocks, or current induced features. The combined analysis of the seismic 3D-data and the cores will help to distinguish between these possibilities.

Another set of cores (M862-14-19, see Fig. 17 for location) were taken along a profile crossing a landslide scar area in the 3D-box).

Two cores (M862-17, 18) were taken on small cone like features close to the coast in order to check, whether these cones are small mud volcanoes. Core recovery of these features was zero

both for the gravity corer and the giant box corer; hence it is unlikely that these features are typical mud volcanoes; they may represent carbonate mounds but we had no tools for sampling or direct video observations during the cruise.

Coring in the Messina Straits was limited due to severe restrictions by the local authorities. In our notification of proposed research we listed 29 possible coring locations for the Messina Straits but only 4 of them were approved mainly due to a dense net of submarine cables in the Messina Straits. All of these locations were in the southernmost part of the Messina Straits at the thalweg of the Messina Canyon. We tried to take gravity cores at the approved locations (M862-23 -26, see Fig. 13 for location) but we did not recover any sediments in the gravity core most likely due to a very sandy canyon floor. Finally we took one giant box core (M862-26). This box core showed the expected sandy sediments but also manmade garbage such as plastic pieces.

5.5.3. First Results

Sediment Core M86/2-007

Sediment core M86/2-007 (Fig. 36) was recovered with a total length of 433 cm in the 3D-survey area. It reveals an inhomogeneous transect through the sediment column. Major tephra layers can be observed at 20-22 cm, 58-61 cm and 325-331 cm. In addition two chaotic units with intraclasts of up to 6 cm can be identified. These units represent mass transported deposits, as they show chaotic internal structures, as well as a mixture of different grain sizes. The section from 325-370 cm bears a tephra layer with a thickness of ca. 6 cm, which is directly underlain by a ca. 40 cm thick chaotic unit. This feature might indicate that a landslide was triggered immediately before or during an eruption and covered by the subsequent fall out of tephra.

Fig. 36 Sediment core M86/2-007 with a total length of 433 cm. The core was taken in the 3D-survey area. See Fig 17 for location of core.

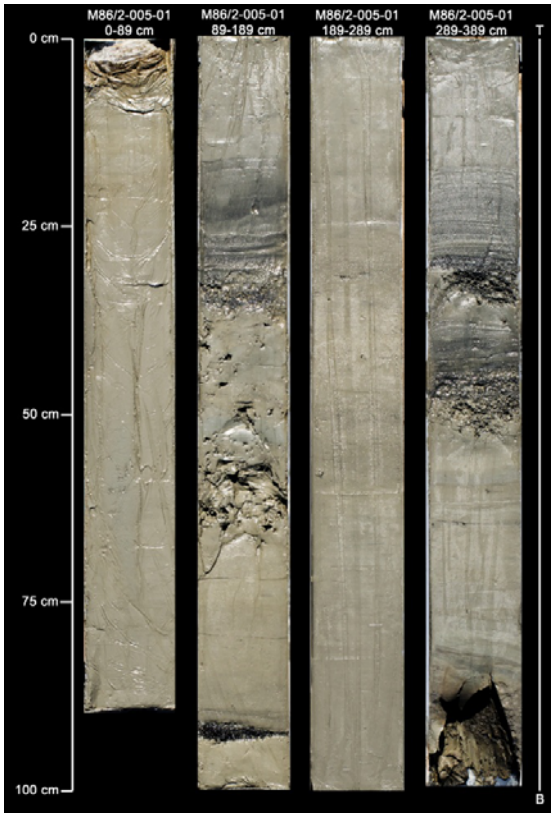

Fig. 37 Sediment core M86/2-005 with a total length of 489 cm recovered from a small basin beneath a major amphitheater-like incision. See Fig. 17 for location of core.

Sediment Core M86/2-005

Sediment core M86/2-005 (Fig. 37) was recovered with a total length of 389 cm in the flat depression surrounded by an amphitheater-like structure (see also Fig. 4). In general, the gravity core shows normal background hemipelagic deposits with grain sizes varying from clay to silt and fine sand. Major volcanic tephra layers a found from 104-125 cm, 177-180 cm and 309-344 cm. A sedimentary unit with coarser material is identified from 139-154 cm. This unit contains pebbles with a grain size of up to 2 cm, most likely deposited by a mass wasting event.

6. Ship's Meteorological Station

(B. Frey, J. Hempelt)

The research vessel Meteor left port in Cartagena / Spain towards Sicily on 27.12.2011 against 10:00h. The working areas of the cruise were to the north of the Messina Straits in the Gioia Basin, the Messina Straits itself, and just off the coast east of Mount Etna.

A low over northern Africa at the start of the cruise caused some headwind with gusts up to force 8 and a swell of 2 m. While passing off Sardinia we received a strong tail wind from a low pressure area over the Ligurian Sea which gave us just the necessary speed to be safe of bad weather approaching from the northwest with waves up to 6 m and winds of up to 9 Bft. We arrived at our first work area, the Gioia Basin, in calm sea and wind conditions on Dec 30th.

The main working area for the following days (01.01.12 – 05.01.12) was between Messina and Catania, where we had very calm weather and sea conditions. However, from the 4th on, some cumulus congestus and cumulonimbus clouds were associated with some showers.

While the time from Jan 1st to 5th was entirely free of gusts, Jan 6th was filled with many showers and gusts. It became the day with the highest number of gusts on this trip with a total amount of 101 gusts. The strongest one occurred on the morning of Jan 7, measured with 55.3 kn or 10 Bft. The waves reached a height of 2 m at this time.

The working areas for the following days were close to the coast. Both, the number and the strength of the gusts decreased and the sea became calm again. The number of gusts had a range of 3-11 per day; their force was about 8 Bft with a maximum of 9 Bft on the evening of Jan 9th (40.7kn).

During the time from 08.01.12 - 12.01.12, we had mainly light winds; total wave height was about 0.5m.

On the afternoon of January 13th, METEOR operated at a greater distance to the coastline and wind and waves increased significantly (37.7°N, 15.6°E) up to force 7 Bft and 1.5 m, respectively. This situation was not forecasted by any of several German and British forecast models, which all predicted only low wind speeds and wave heights lower than 0.5 m (MSM, GSM, LSM, ESM, ECM).

On the night of 16th to 17th, the scientific program ended and the transit to Brindisi was started. On the morning of January 17th, Cruise M86/2 ended at the port of Brindisi.

7. Station List M86/2

Tab. 2: List of 2D-seismic profiles

METEOR Station	Profil-Nr.	Date	Time Start UTC	Time End UTC	Latitude Start xx° x.x'N	Longitude Start xx° x.x'E	Latitude End xx° x.x'N	Longitude End xx° x.x'E	FFN Start	FFN End
M862/1316-1	101	30.12.2011	18:47	19:31	38:33.60	15:32.30	38:31.23	15:29.76	364	781
M862/1316-1	102	30.12.2011	19:36	20:51	38:30.87	15:30.10	38:29.72	15:36.76	885	1762
M862/1316-1	103	30.12.2011	21:00	22:18	38:30.10	15:37.15	38:35.65	15:36.92	1872	2807
M862/1316-1	104	30.12.2011	22:25	23:35	38:35.94	15:37.45	38:34.22	15:43.51	2894	3775
M862/1316-1	105	31.12.2011	23:35	01:50	38:34.22	15:43.51	38:24.60	15:44.50	2895	5347
M862/1316-1	106	31.12.2011	01:53	04:04	38:24.50	15:44.40	38:15.81	15:39.76	5379	6942
M862/1316-1	107	31.12.2011	04:04	05:27	38:15.81	15:39.76	38:12.52	15:34.25	6942	7943
M862/1316-1	108	31.12.2011	05:27	06:38	38:12.52	15:34.25	38:07.86	15:38.61	7943	8787
M862/1316-1	109	31.12.2011	06:38	06:50	38:07.86	15:38.61	38:06.83	15:38.28	8787	8940
M862/1316-1	110	31.12.2011	06:50	06:52	38:06.83	15:38.28	38:01.83	15:37.66	8940	8990
M862/1316-1	111	31.12.2011	06:52	07:20	38:01.83	15:37.66	38:08.00	15:37.76	8990	9263
M862/1316-1	201	31.12.2011	09:03	09:31	38:07.11	15:37.41	38:09.20	15:38.39	10120	10447
M862/1316-1	202	31.12.2011	09:31	09:39	38:09.20	15:38.39	38:08.99	15:38.84	10447	10504
M862/1316-1	203	31.12.2011	09:39	09:52	38:08.99	15:38.84	38:07.87	15:38.63	10504	10699
M862/1316-1	204	31.12.2011	09:52	10:48	38:07.87	15:38.62	38:10.77	15:34.85	10699	11365
M862/1316-1	205	31.12.2011	10:51	10:59	38:11.05	15:34.96	38:11.56	15:35.45	11398	11508
M862/1316-1	206	31.12.2011	11:06	11:40	38:11.20	15:35.67	38:09.59	15:34.28	11570	11890
M862/1316-1	207	31.12.2011	11:45	12:27	38:09.30	15:34.39	38:07.09	15:37.53	11926	12436
M862/1316-1	208	31.12.2011	12:43	13:13	38:07.22	15:36.85	38:09.45	15:37.37	12527	12892
M862/1316-1	209	31.12.2011	13:27	13:56	38:09.00	15:37.78	38:08.75	15:34.58	13052	13421
M862/1316-1	210	31.12.2011	14:04	14:30	38:08.38	15:34.55	38:07.64	15:37.02	13495	13808
M862/1316-1	211	31.12.2011	14:38	14:48	38:07.20	15:36.82	38:07.03	15:35.88	13905	14024
M862/1316-1	212	31.12.2011	14:53	15:50	38:07.33	15:35.81	38:11.71	15:36.60	14080	14768
M862/1316-1	213	31.12.2011	15:50	16:02	38:11.71	15:36.60	38:12.10	15:35.49	14768	14911
M862/1316-1	214	31.12.2011	16:02	16:25	38:12.10	15:35.49	38:10.29	15:34.04	14911	15188
M862/1316-1	215	31.12.2011	16:30	17:16	38:10.05	15:34.28	38:07.38	15:37.72	15235	15819
M862/1316-1	216	31.12.2011	17:16	17:32	38:07.38	15:37.72	38:06.15	15:37.41	15819	16000
M862/1316-1	217	31.12.2011	17:40	18:43	38:06.22	15:37.03	38:08.88	15:33.00	16091	16839
M862/1316-1	218	31.12.2011	18:47	18:53	38:08.74	15:32.68	38:08.36	15:32.38	16893	16963
M862/1316-1	219	31.12.2011	18:57	20:05	38:08.11	15:32.54	38:04.06	15:37.69	17014	17845
M862/1316-1	220	31.12.2011	20:05	20:12	38:04.06	15:37.69	38:03.46	15:37.44	17845	17937
M862/1316-1	221	31.12.2011	20:12	20:29	38:03.46	15:37.44	38:04.05	15:36.07	17937	18143
M862/1316-1	222	31.12.2011	20:29	21:10	38:04.05	15:36.07	38:07.15	15:36.75	18143	18614
M862/1316-1	223	31.12.2011	21:15	21:51	38:07.41	15:36.46	38:08:58	15:33.76	18664	18993
M862/1316-1	224	31.12.2011	21:55	22:27	38:08.45	15:33.42	38:06.43	15:31.35	19164	19557
M862/1316-1	225	31.12.2011	22:33	23:30	38:06.21	15:31.52	38:03.90	15:36.15	19601	20264
M862/1316-1	226	31.12.2011	23:33	23:43	38:03.59	15:35.39	38:03.35	15:35.10	20325	20444
M862/1316-1	227	01.01.2012	23:47	00:30	38:03.63	15:35.05	38:07.00	15:35.63	20503	21014
M862/1316-1	228	01.01.2012	00:35	01:00	38:07.03	15:35.21	38:06.32	15:31.23	21051	21551
M862/1316-1	229	01.01.2012	01:05	01:50	38:06.10	15:31.11	38:03.50	15:30.08	21554	21993

METEOR Station	Profil-Nr.	Date	Time Start	Time End	Latitude Start	Longitude Start	Latitude End	Longitude End	FFN Start	FFN End
			UTC	UTC	xx° x.x‘N	xx° x.x‘E	xx° x.x‘N	xx° x.x‘E		
M862/1316-1	230	01.01.2012	01:53	03:16	38:03.08	15:30.31	38:00.83	15:37.78	22060	23003
M862/1316-1	231	01.01.2012	03:33	05:10	37:59.89	15:37.46	38:01.25	15:27.61	23200	24368
M862/1316-1	232	01.01.2012	05:13	05:27	38:01.07	15:27.45	38:00.05	15:27.04	24412	24578
M862/1316-1	233	01.01.2012	05:31	07:31	37:59.89	15:27.31	37:57.38	15:39.02	24621	26083
M862/1316-1	234	01.01.2012	07:31	10:45	37:57.38	15:39.02	37:42.15	15:41.96	26083	28388
M862/1316-1	235	01.01.2012	10:45	10:59	37:42.15	15:41.96	37:42.36	15:43.10	28388	28568
M862/1316-1	236	01.01.2012	10:59	12:24	37:42.36	15:43.10	37:49.05	15:41.81	28568	29583
M862/1316-1	237	01.01.2012	12:28	12:59	37:49.07	15:41.41	37:48.43	15:38.60	29630	29997
M862/1316-1	238	01.01.2012	13:02	14:17	37:48.16	15:38.44	37:42.25	15:40.07	30014	30916
M862/1316-1	239	01.01.2012	14:23	14:35	37:41.96	15:39.82	37:41.87	15:38.80	30983	31126
M862/1316-1	240	01.01.2012	14:40	16:26	37:42.06	15:38.57	37:50.06	15:36.15	31186	32463
M862/1316-1	241	01.01.2012	16:43	17:15	37:50.61	15:35.51	37:50.47	15:32.44	32655	33041
M862/1316-1	242	01.01.2012	17:20	18:47	37:50.01	15:32.34	37:42.85	15:32.45	33106	34154
M862/1316-1	243	01.01.2012	18:52	21:42	37:42.62	15:32.08	37:38.64	15:14.62	34212	36273
M862/1316-1	244	01.01.2012	21:42	23:18	37:38.64	15:14.62	37:31.31	15:11.22	36273	37385
M862/1316-1	245	01.01.2012	23:23	23:44	37:31.11	15:11.57	37:30.65	15:13.63	37460	37718
M862/1316-1	246	02.01.2012	23:49	03:30	37:30.89	15:14.00	37:47.24	15:21.97	37777	40434
M862/1316-1	247	02.01.2012	03:35	04:00	37:47.33	15:22.43	37:47.06	15:24.53	40480	40783
M862/1316-1	248	02.01.2012	04:06	06:30	37:46.68	15:24.67	37:35.47	15:19.46	40862	42576
M862/1316-1	249	02.01.2012	06:35	06:55	37:35.16	15:19.61	37:34.38	15:21.55	42627	42872
M862/1316-1	250	02.01.2012	07:01	07:09	37:34.67	15:22.00	37:35.27	15:22.37	42939	43033
M862/1316-1	251	02.01.2012	07:15	07:49	37:35.64	15:22.10	37:37.07	15:18.84	43097	43525
M862/1316-1	301	02.01.2012	11:00	11:58	37:36.80	15:19.91	37:39.37	15:15.07	44083	44760
M862/1316-1	302	02.01.2012	12:04	12:26	37:39.30	15:14.37	37:38.38	15:12.54	44827	45107
M862/1316-1	303	02.01.2012	12:36	14:39	37:38.83	15:12.13	37:48.17	15:16.16	45233	46693
M862/1316-1	304	02.01.2012	14:45	15:05	37:48.30	15.16.65	37:47.99	15:18.67	46761	47005
M862/1316-1	305	02.01.2012	15:11	17:02	37:47.63	15:18.87	37:38.94	15:14.57	47075	48404
M862/1316-1	306	02.01.2012	17:09	17:28	37:38.97	15:14.05	37:40.29	15:13.04	48492	48718
M862/1316-1	307	02.01.2012	17:31	17:50	37:40.50	15:12.98	37:41.53	15:13.25	48752	48983
M862/1316-1	401	02.01.2012	19:31	22:01	37:41.14	15:16.83	37:33.76	15:29.47	50002	51800
M862/1316-1	402	02.01.2012	22:05	22:23	37:33.92	15:29.81	37:35.24	15:30.82	51854	52070
M862/1316-1	403	02.01.2012	22:29	23:43	37:35.57	15:30.63	37:39.04	15:24.53	52132	53010
M862/1316-1	404	03.01.2012	23:53	01:52	37:39.71	15:24.60	37:48.36	15:28.40	53122	54553
M862/1316-1	405	03.01.2012	01:58	02:17	37:48.46	15:28.94	37:48.00	15:30.67	54630	54843
M862/1316-1	406	03.01.2012	02:23	05:17	37:47.58	15:30.63	37:38.00	15:26.38	54922	56423
M862/1316-1	407	03.01.2012	05:20	08:10	37:38.06	15:26.23	37:45.25	15:13.68	56463	58521
M862/1316-1	408	03.01.2012	08:16	08:41	37:45.53	15:13.80	37:47.16	15:15.13	58587	58880
M862/028-1	601	12.01.2012	16:03	16:31	37:41.45	15:16.26	37:42.91	15:14.20	100	619
M862/028-1	602	12.01.2012	16:35	17:22	37:43.22	15:14.33	37:45.21	15:18.40	686	1394
M862/028-1	603	12.01.2012	17:30	17:48	37:45.60	15:18.21	37:46.08	15:16.41	1504	1784
M862/028-1	604	12.01.2012	17:53	20:35	37:45.86	15:16.10	37:32.99	15:10.49	1854	4308
M862/028-1	605	12.01.2012	20:41	21:01	37:32.60	15:10.73	37:32.23	15:12.57	4400	4673
M862/028-1	606	12.01.2012	21:06	22:46	37:32.51	15:12.94	37:40.23	15:16.51	4746	6250

METEOR Station	Profil-Nr.	Date	Time Start	Time End	Latitude Start	Longitude Start	Latitude End	Longitude End	FFN Start	FFN End
			UTC	UTC	xx° x.x‘N	xx° x.x‘E	xx° x.x‘N	xx° x.x‘E		
M862/028-1	701	13.01.2012	22:56	01:42	37:40.31	15:17.42	37:39.06	15:34.83	6500	8166
M862/028-1	702	13.01.2012	01:47	02:19	37:38.76	15:35.00	37:36.06	15:35.10	8216	8537
M862/028-1	703	13.01.2012	02:24	04:31	37:35.88	15:34.71	37:36.36	15:21.45	8593	9864
M862/028-1	704	13.01.2012	04:38	06:44	37:35.92	15:21.54	37:30.17	15:32.39	9926	11180
M862/028-1	705	13.01.2012	06:47	07:02	37:30.24	15:32.78	37:31.19	15:33.64	11222	11366
M862/028-1	706	13.01.2012	07:07	07:23	37:31.54	15:33.43	37:32.30	15:32.08	11419	11576
M862/028-1	801	13.01.2012	08:24	08:48	37:32.15	15:32.34	37:33.23	15:30.44	12180	12425
M862/028-1	802	13.01.2012	08:59	10:40	37:33.91	15:29.72	37:42.26	15:31.21	12538	13543
M862/028-1	803	13.01.2012	10:43	11:40	37:42.55	15:31.24	37:47.45	15:31.23	13576	14157
M862/028-1	804	13.01.2012	11:44	12:12	37:47.63	15:31.52	37:48.15	15:34.34	14197	14487
M862/028-1	805	13.01.2012	12:17	13:20	37:47.85	15:34.68	37:42.85	15:35.91	14542	15135
M862/028-1	806	13.01.2012	13:23	13:33	37:42.75	15:36.25	37:42.86	15:37.17	15180	15277
M862/028-1	807	13.01.2012	13:38	14:36	37:43.17	15:37.31	37:47.99	15.35.92	15322	15903
M862/028-1	808	13.01.2012	14:41	14:54	37:48.27	15:36.59	37:48.20	15:37.56	15955	16075
M862/028-1	809	13.01.2012	14:57	15:54	37:48.02	15:37.63	37:43.30	15:38.94	16114	16691
M862/028-1	810	13.01.2012	16:13	16:54	37:43.62	15:40.34	37:47.12	15:39.64	16878	17290
M862/028-1	811	13.01.2012	16:58	17:38	37:47.73	15:39.74	37:50.57	15:41.26	17323	17725
M862/028-1	812	13.01.2012	17:43	20:23	37:50.89	15:40.87	37:50.34	15:23.30	17781	19394
M862/028-1	900	13.01.2012	20:31	21:29	37:50.93	15:23.07	37:55.46	15:24.50	20000	20675
M862/028-1	901	13.01.2012	21:34	22:20	37:55.61	15:24.96	37:55.06	15:30.71	20736	21292
M862/028-1	902	13.01.2012	22:24	23:02	37:55.20	15:30.41	37:56.90	15:33.49	21338	21800
M862/028-1	903	14.01.2012	23:07	00:04	37.57.43	15:33.93	38:02.22	15:34.26	21840	22556
M862/028-1	904	14.01.2012	00:05	00:34	38:02.23	15:34.30	38:04.52	15:35.39	22560	22913
M862/028-1	905	14.01.2012	00:36	00:51	38:04.63	15:35.37	38:05.88	15:34.62	22929	23117
M862/028-1	906	14.01.2012	00:55	01:06	38:05.99	15:34.16	38:05.79	15:33.14	23170	23295
M862/028-1	907	14.01.2012	01:10	01:30	38:05.53	15:32.95	38:03.78	15:32.80	23344	23591
M862/028-1	908	14.01.2012	01:32	02:44	38:03.70	15:32.75	37:59.01	15:34.77	23602	24436
M862/028-1	909	14.01.2012	02:44	03:28	37:58.83	15:29.82	37:59.01	15:34.77	24436	24981
M862/028-1	910	14.01.2012	03:28	03:49	37:59.01	15:34.77	38:00.12	15:36.31	24981	25233
M862/028-1	911	14.01.2012	03:49	04:23	38:00.12	15:36.31	38:02.92	15:37.43	25233	25644
M862/028-1	912	14.01.2012	04:23	04:58	38:02.92	15:37.43	38:05.87	15:37.19	25644	26062
M862/028-1	1000	14.01.2012	05:01	05:46	38:06.16	15:37.32	38:09.60	15:38.73	27000	27681
M862/028-1	1001	14.01.2012	05:46	06:32	38:09.60	15:38.73	38:12.28	15:36.37	27681	28376
M862/028-1	1002	14.01.2012	06:46	07:33	38:11.74	15:35.55	38:08.53	15:38.48	28597	29306
M862/028-1	1003	14.01.2012	07:42	07:54	38:08.94	15:38.65	38:09.72	15:37.82	29436	29612
M862/028-1	1004	14.01.2012	07:58	08:51	38:09.62	15:37.42	38:06.69	15:33.11	29676	30462
M862/028-1	1005	14.01.2012	08:57	09:08	38:06.26	15:33.21	38:05.70	15:34.32	30559	30713
M862/028-1	1006	14.01.2012	09:11	09:48	38:05.84	15:34.55	38:07.83	15:37.52	30787	31346
M862/028-1	1007	14.01.2012	09:51	10:32	38:08.12	15:37.50	38:11.46	15:37.25	31401	32013
M862/028-1	1008	14.01.2012	10:44	11:18	38:11.05	15:37.49	38:09.52	15:34.64	32186	32670
M862/028-1	1009	14.01.2012	11:18	12:04	38:09.52	15:34.64	38:06.42	15:31.85	32670	33355
M862/028-1	1010	14.01.2012	12:04	12:19	38:06.42	15:31.85	38:05.15	15:31.30	33355	33589
M862/028-1	1011	14.01.2012	12:51	13:35	38:06.62	15:31.41	38:09.95	15:33.50	33622	34316

METEOR Station	**Profil-Nr.**	**Date**	**Time Start**	**Time End**	**Latitude Start**	**Longitude Start**	**Latitude End**	**Longitude End**	**FFN Start**	**FFN End**
			UTC	**UTC**	**xx° x.x‘N**	**xx° x.x‘E**	**xx° x.x‘N**	**xx° x.x‘E**		
M862/028-1	1012	14.01.2012	13:35	14:24	38:09.95	15:33.50	38:11.79	15:36.82	34316	35043
M862/028-1	1013	14.01.2012	14:24	14:54	38:11.79	15:36.82	38:13.90	15:37.38	35043	35495
M862/028-1	1014	14.01.2012	14:54	16:01	38:13.90	15:37.38	38:15.54	15:42.22	35495	36484
M862/028-1	1015	14.01.2012	16:01	16:09	38:15.54	15:42.22	38:16.10	15:42.41	36484	36590
M862/028-1	1016	14.01.2012	16:17	16:25	38:15.88	15:43.02	38:15.39	15:42.59	36713	36836
M862/028-1	1017	14.01.2012	16:25	16:31	38:15.39	15:42.59	38:15.34	15:42.07	36836	36919
M862/028-1	1018	14.01.2012	16:35	17:02	38:15.59	15:41.86	38:17.37	15:41.36	36983	37400
M862/028-1	1019	14.01.2012	17:02	17:24	38:17.37	15:41.36	38:17.60	15:39.28	37400	37728
M862/028-1	1020	14.01.2012	17:30	17:57	38:17.23	15:39.15	38:15.49	15:40.84	37805	38210
M862/028-1	1021	14.01.2012	18:00	18:20	38:15.51	15:41.55	38:16.25	15:43.04	38263	38562
M862/028-1	1022	14.01.2012	18:20	19:08	38:16.25	15:43.04	38:18.13	15:48.02	38562	39307
M862/028-1	1023	14.01.2012	19:12	19:37	38:18.23	15:48.08	38.20.30	15:49.41	39440	39743
M862/028-1	1024	14.01.2012	19:43	20:20	38:20.73	15:49.07	38:21.18	15:45.24	39859	40394
M862/028-1	1025	14.01.2012	20:25	20:37	38:20.94	15:44.89	38:19.92	15:44.41	40471	40652
M862/028-1	1026	14.01.2012	20:40	21:13	38:19.75	15:44.58	38:17.76	15:46.89	40692	41161
M862/028-1	1027	14.01.2012	21:20	21:29	38:17.87	15:47.40	38:18.62	15:48.03	41259	41404
M862/028-1	1028	14.01.2012	21:32	22:11	38:18.78	15:48.11	38:22.15	15:49.31	41437	42020
M862/028-1	1029	14.01.2012	22:13	23:40	38:22.29	15:49.39	38:29.01	15:53.96	42055	43376
M862/028-1	1030	15.01.2012	23:46	01:40	38:29.32	15:53.64	38:32.58	15:41.53	43455	45165
M862/028-1	1031	15.01.2012	01:45	02:07	38:32.88	15:41.51	38:34.61	15:42.67	45233	45560
M862/028-1	1032	15.01.2012	02:10	03:29	38:34.65	15:42.99	38:32.65	15:51.34	45619	46795
M862/028-1	1033	15.01.2012	03:33	06:14	38:32.34	15.51:47	38:18.86	15:47.79	46854	49273
M862/033-1	1101	15.01.2012	16:00	17:59	38:01.74	15:37.96	38:04.38	15:30.60	50010	51456
M862/033-1	1102	15.01.2012	18:06	18:30	38:04.10	15:30.36	38:02.20	15:29.48	51525	51831
M862/033-1	1103	15.01.2012	18:36	19:46	38:01.92	15:29.82	38:00.24	15:37.31	51900	52754
M862/033-1	1104	15.01.2012	19:49	20:01	37:59.95	15:37.44	37:58.82	15:37.31	52801	52970
M862/033-1	1105	15.01.2012	20:08	20:23	37:58.82	15:36.82	37:59.10	15:35.24	53020	53198
M862/033-1	1106	15.01.2012	20:28	22:21	37:58.79	15:34.99	37:47.88	15:33.84	53258	54594
M862/033-1	1107	15.01.2012	22:25	22:58	37:48.72	15:33.48	37:48.21	15:29.81	54640	55043
M862/033-1	1108	16.01.2012	23:02	01:02	37:48.47	15:29.59	37:59.16	15:29.43	55106	56524

Tab. 3: List of stations
SVP: Sound Velocity Profiler
GKG: Giant Box Corer
SL: Gravity Corer

METEOR Station	Core Station	Lat	Lon	Water Depth [m]	Gear	Recovery [m]
M862/1313-1	M86/2-001-01	38:35.04	15:33.71	930	SVP	
M862/1313-2	M86/2-001-02	38:35.04	15:33.73	939	GKG	0.53
M862/1313-3	M86/2-001-03	38:35.03	15:33.73	936	SL	3.82
M862/1314-1	M86/2-002-01	38:36.48	15:35.51	885	SL	4.91
M862/1315-1	M86/2-003-01	38:37.95	15:37.28	742	SL	3.82
M862/002-1	M86/2-004-01	37:40.36	15:21.99	1554	SL	3.38
M862/003-1	M86/2-005-01	37:40.77	15:21.47	1560	SL	3.89
M862/004-1	M86/2-006-01	37:40.33	15:22.33	1546	SL	4.77
M862/005-1	M86/2-007-01	37:39.58	15:16.48	689	SL	4.33
M862/006-1	M86/2-008-01	37:39.63	15:16.71	650	SL	4.95 (surface missing (~8cm)
M862/007-1	M86/2-009-01	37:39.57	15:16.34	680	SL	2.21
M862/008-1	M86/2-010-01	37:39.53	15:16.14	724	SL	only core catcher
M862/010-1	M86/2-011-01	37:41.41	15:26.71	1877	SL	2.23
M862/011-1	M86/2-012-01	37:40.35	15:21.59	1562	SL	2.66
M862/012-1	M86/2-013-01	37:40.44	15:21.00	1565	SL	4.35
M862/017-1	M86/2-014-01	37:41.23	15:15.76	486	SL	4.51
M862/018-1	M86/2-015-01	37:41.56	15:15.90	460	SL	3.56
M862/019-1	M86/2-016-01	37:41.91	15:16.08	448	SL	5 (surface missing)
M862/020-1	M86/2-016-02	37:41.91	15:16.08	447	SL	7.84
M862/020-2	M86/2-017-01	37:46.24	15:14.57	84	SL	0.00
M862/020-3	M86/2-017-02	37:46.23	15:14.50	83	GKG	0.00
M862/020-4	M86/2-017-03	37:46.23	15:14.50	82	GKG	0.00
M862/021-1	M86/2-018-01	37:46.24	15:14.51	85	SL	0.00
M862/024-1	M86/2-019-01	37:42.25	15:16.25	462	SL	7.53
M862/025-1	M86/2-020-01	37:40.25	15:15.27	609	SL	4.52
M862/026-1	M86/2-021-01	37:40.46	15:15.39	613	SL	0.00
M862/027-1	M86/2-022-01	37:40.17	15:16.80	630	SL	4.60
M862/029-1	M86/2-023-01	38:03.35	15:33.66	1088	SL	0.00
M862/030-1	M86/2-024-01	37:57.94	15:31.57	1333	SL	0.00
M862/031-1	M86/2-025-01	37:57.71	15:31.24	1307	SL	0.00
M862/032-1	M86/2-026-01	38:01.85	15:33.17	1175	GKG	0.30

Tab. 4: Deployed OBS in the 3D-cube (Ship's station Number M862/013-1)

OBS-Nr.	Lat	Lon
501	37°41.25'N	15°15.79'E
502	37°39.52'N	15°14.81'E
503	37°38.95'N	15°16.31'E
504	37°40.80'N	15°17.38'E

8. Data and Sample Storage and Availability

All meta-data of the cruise were made available immediately after the cruise via the Kiel data portal for marine science (https://portal.geomar.de/web/guest/kdmi).
The seismic, bathymetric and hydro-acoustic raw data as well as processed seismic data are archived on a dedicated server at GEOMAR (Server Permian operated by the GEOMAR Data and Computing Centre). The GEOMAR server Permian is daily backed up and holds all data since the founding days of IFM-GEOMAR/GEOMAR. The acoustic data will be submitted to a public data base as soon such a data base for long-term archival will be available and standards for archiving have been defined. The moratorium for exclusive use by M86/2 scientists is set to three years until February 1st, 2015. Thereafter the data will be available for other scientists upon request. Person to contact is Professor S. Krastel.

All cores are stored and archived in the Kiel core repository. The M86/2 scientific party has a three-year moratorium time until February 1st, 2015, for exclusive analytical work before the cores will be available for sampling by other scientists upon reasonable statement. All data measured at the cores during the and post cruise will be included in the PANGAEA data base in Bremerhaven, which will then provide long-term archival and access to the data within WDC-MARE.

9. Acknowledgements

The scientific party of Meteor Cruise M86/2 gratefully acknowledges the very friendly and most effective cooperation with Captain Schneider and his crew. Their perfect technical assistance in a difficult working area substantially contributed to make this cruise a scientific success. Local authorities including Messina VTS, Messina Pilots, Messina Harbor Master, Marisicilia, Compamare Catania, and the coast guard are thanked for the very good and efficient communication and support allowing us to run all lines as planned. We also appreciate the valuable support by the Leitstelle Deutsche Forschungsschiffe at the University of Hamburg. This expedition was funded by the Deutsche Forschungsgemeinschaft (DFG) and the Bundesministerium für Bildung und Forschung (BMBF).

10. References

Argnani, A., Brancolinib, G., Bonazzia, C., Roverea, M., Accainob, F., Zgurb, F., Lodolob, E. (2009a) The results of the Taormina 2006 seismic survey: Possible implications for active tectonics in the Messina Straits. Tectonophysics, 476, 159-169.

Argnani, A., Chiocci, F.L., Tinti, S., Bosmann, A., Lodi, M.V., Pagnoni, G., Zaniboni, F. (2009b). Comment on "On the cause of the 1908 Messina tsunami, southern Italy" by Andrea Billi et al. Geophysical Research Letters, 36, L13307, doi:10.1029/2009GL037332.

Baratta, M. (1910) La catastrophe sismica calabro-messinese. 28 Dicembre 1908. Societa Geografica Italiana, Roma, 2 Volumes, pp. 426.

Bialas, J., Flueh, E.R., (1999) A new Ocean Bottom Seismometer (with a new type of data logger). Sea Technology, Vol. 40, 4, 41-46

Billi, A., Funiciello, R., Minelli, L., Faccenna, C., Neri, G., Orecchio, B., Presti, D. (2008) On the cause of the 1908 Messina tsunami, southern Italy. Geophysical Research Letters, 35, L06301, doi:10.1029/2008GL033251

dos Santos, C., Quadfasel, D., Stokland, G., Rogenahgen, J. (2011). Kongsberg EM122 and EM710. Quick manual

Flueh, E.R., Bialas, J. (1996) A digital, high data capacity ocean bottom recorder for marine seismic investigations. Underwater Systems Design, 18/3, 18-20

Gamberi, F., Marani, M. (2008) Controls on Holocene deep-water sedimentation in the northern Gioia Basin, Tyrrhenian Sea. Sedimentology, 55, 1889-1903.

Marani, M. P., Gamberi, F., Bortoluzzi, G., Carrara, G., Ligi, M., Penitenti, D. (2004) Seafloor bathymetry of the Ionian Sea. In Marani, M. P., Gamberi, F., Bonatti, E. (eds) From seafloor to deep mantle: architecture of the Tyrrhenian backarc basin, Mem. Descr. Carta Geol. It., 44, Plate 3.Platania, G. (1909) Il maremoto dello Stretto di Messina del 28 Dicembre 1908, Boll. Soc. Sismol. It., 13, 369– 458.

Pareschi, M.T., Boschi, E., Favalli, M. (2006a) The lost tsunami. Geophys. Res. Lett., 33, L22608, doi:10.1029/2006GL026064.

Pareschi, M. T., Boschi, E. Mazzarini, F., Favalli, M. (2006b) Large submarine landslides offshore Mt. Etna, Geophys. Res. Lett., 33, L13302, doi:10.1029/2006GL026064.

Scrocca, D., et al. (eds) (2004) CROP Atlas, Ist. Super. Per la Prot. E la Ric., Ambientale, Rome, 197 pp.

Vigliotto, L. (2008) Comment on ‘‘Lost tsunami’’ by Maria Teresa Pareschi et al. Gepophys. Res. Lett., 35, L02608, doi:10.1029/2007GL031155.